AD NUMBER

ADB328711

NEW LIMITATION CHANGE

TO

Approved for public release, distribution unlimited

FROM

Distribution authorized to U.S. Gov't. agencies only; Proprietary Information; FEB 2007. Other requests shall be referred to U.S. Army Research Office, P.O. Box 12211, Research Triangle Park, NC 27709-2211.

AUTHORITY

28 Feb 2007, per document marking

REPORT DOCUMENTATION PAGE

Form Approved OMB NO. 0704-0188

1. AGENCY USE ONLY (Leave Blank)	2. REPORT DATE:	3. REPORT TYPE AND DATES COVERED
		Final Report 1-Jun-2001 - 30-Nov-2006

4. TITLE AND SUBTITLE

Science and Technology of Chemicals and Biological Sensing at Terahertz Frequencies

5. FUNDING NUMBERS

DAAD19-01-1-0622

6. AUTHORS

Tatiana Globus, Robert M. Weikle, II, Elliott Brown, Jack East

8. PERFORMING ORGANIZATION REPORT NUMBER

7. PERFORMING ORGANIZATION NAMES AND ADDRESSES

University of Virginia
Office of Sponsored Programs
1001 N. Emmett St. P.O. Box 400195
Charlottesville, VA 22904 -4195

9. SPONSORING/MONITORING AGENCY NAME(S) AND ADDRESS(ES)

U.S. Army Research Office
P.O. Box 12211
Research Triangle Park, NC 27709-2211

10. SPONSORING / MONITORING AGENCY REPORT NUMBER

42214-EL-MUR.5

11. SUPPLEMENTARY NOTES

The views, opinions and/or findings contained in this report are those of the author(s) and should not contrued as an official Department of the Army position, policy or decision, unless so designated by other documentation.

12. DISTRIBUTION AVAILIBILITY STATEMENT

Approved for Public Release; Distribution Unlimited

12b. DISTRIBUTION CODE

13. ABSTRACT (Maximum 200 words)

The abstract is below since many authors do not follow the 200 word limit

14. SUBJECT TERMS

Terahertz, Biological Agents, Spectroscopy

15. NUMBER OF PAGES

Unknown due to possible attachments

16. PRICE CODE

17. SECURITY CLASSIFICATION OF REPORT	18. SECURITY CLASSIFICATION ON THIS PAGE	19. SECURITY CLASSIFICATION OF ABSTRACT	20. LIMITATION OF ABSTRACT
UNCLASSIFIED	UNCLASSIFIED	UNCLASSIFIED	UL

NSN 7540-01-280-5500

Standard Form 298 (Rev .2-89)
Prescribed by ANSI Std.
239-18 298-102

Report Title

Science and Technology of Biological and Chemical Sensing at
Terahertz Frequencies

ABSTRACT

This research program is aimed to discover and understand the fundamental physical principles governing the interaction of biological molecules with electromagnetic radiation in the terahertz region of the spectrum. In addition, a critical focus is to develop the technology needed to study these interactions and to apply this technology to the design and realization of instrumentation for detecting and identifying biological molecules and their agents. Achieving these objectives is a vital concern for both military and civilian authorities as they address the potential threat of biological and chemical warfare. It is the aim of this program to develop the science and technology needed to meet these goals.

List of papers submitted or published that acknowledge ARO support during this reporting period. List the papers, including journal references, in the following categories:

(a) Papers published in peer-reviewed journals (N/A for none)

R. Parthasarathy, T. Globus, T. Khromova, N. Swami, D. Woolard, “Dielectric properties of biological molecules in the Terahertz gap”, J.Appl. Phys. Lett., v. 87, 11, 2005.

T.Globus,D.Woolard,T.W.Crowe, T.Khromova, B. Gelmont, J. Hessler, “Terahertz Fourier transform characterization of biological materials in a liquid phase”, J. Phys. D: Appl. Phys. 39 3405-3413 (2006).

D. L. Woolard, Y. Luo, B. L. Gelmont, T. Globus and J. O. Jensen, “Bio-molecular inspired electronic architectures for enhanced sensing of thz-frequency bio-signatures”, International Journal of
High Speed Electronics and Systems (IJHSES), Vol.20, No. 10, 1-15 (2005).

“Analysis and Design of Si Terahertz Transit Time Devices”, X. Bi, J. East U. Ravaioli and G. Haddad, Solid State Electronics, Issue 5, May 2006, pages 889-896.

“Optical Attenuation Signatures of Bacillus Subtilis in the THz Region,” E.R. Brown, J.E. Bjarnason, T.L.J. Chan, A.W.M. Lee, and M.A. Celis, Appl. Phys. Lett., vol. 84 (no 18), p 3438-3440.

"Millimeter-wave, terahertz, and mid-infrared transmission through common clothing" , J. E. Bjarnason, T. L. J. Chan, A. W. M. Lee, M. A. Celis, and E. R. Brown, Appl. Phys. Lett. vol. 85 (no. 4), pp. 519-521. [2004]

“Attenuation contrast between biomolecular and inorganic materials at terahertz frequencies, T. L. J. Chan, J. E. Bjarnason, A. W. M. Lee, M. A. Celis, and E. R. Brown., Appl. Phys. Lett., vol. 85 (no.
13), pp. 2523-2525.. [2004]

“ErAs:GaAs photomixer with two-decade tunability and 12 μW peak output power,” J. E. Bjarnason, T. L. J. Chan, A. W. M. Lee, E. R. Brown, D. C. Driscoll, M. Hanson, A. C. Gossard, and R. E. Muller, Appl. Phys. Lett. , vol. 85 (no 18), p. 3983 [2004].

“Room temperature, THz photomixing sweep oscillator and its application to spectroscopic transmission through organic materials”, E. R. Brown, J. Bjarnason, T. L. J. Chan, D. C. Driscoll, M. Hanson, and A. C. Gossard, Rev. Sci. Inst., vol. 75 (no. 12) p. 5333 [2004]

“Bright MM-Wave and THz Luminescence by Down-Conversion of near-IR Amplified-Spontaneous-Emission,” E.R. Brown, J. E. Bjarnason, T.L.J. Chan, D. C. Driscoll, M. Hanson, and A.C. Gossard, Int. J. Infrared and MM Waves, Vol. 26, No. 12, pp. 1691-1702 (2005)

“Terahetz Frequency Sensing and Imaging: A Time of Reckoning Future Applications,” D.L. Woolard, E.R. Brown, M. Pepper, and M. Kemp, “Proc. IEEE, vol 93, (no 10), Oct. 2005.

“Sensitivity measurement and analysis of an ErAs:GaAs coherent photomixing transceiver,” J.E. Bjarnason and E.R. Brown, Appl. Phys. Lett., Vol. 87, 134105 (2005).

“THz Regime Attenuation Signatures in Bacillus subtilis and a Model Based on Surface Polariton Effects,” E.R. Brown, T.B. Khromova, T. Globus, D.L. Woolard, J.O. Jensen, and A. Majewski, IEEE Sensors J., Vol. 6, No. 5, pp. 1076-1083 (2006).

"0.15-3.72 THz absorption of aqueous salts and saline solutions," J. Xu, K. W. Plaxco, S. J. Allen,, J. E. Bjarnason, E. R. Brown, Appl. Phys. Lett, 90, 031908 (2007).

“On the Strong and Narrow Absorption Signature in Lactose at 0.53 THz,” E.R. Brown, J.E. Bjarnason, A.M. Fedor, and T.M. Korter Appl. Phys. Lett., vol. 90 061908 (2007).

H. Xu, G.S. Schoenthal, J.L. Hesler, T.W. Crowe, and R.M. Weikle, II, “Non-Ohmic Contact Planar Varactor Frequency Upconverters for Terahertz Applications,” to be published in the IEEE
Trans. Microwave and Tech., April 2007.

H. Xu, Y. Duan, J.L. Hesler, T.W. Crowe, and R.M. Weikle, II, “Subharmonically-pumped millimeter-wave upconverters based on heterostructure barrier varactors," IEEE Trans. Microwave Theory and Tech., vol. MTT-54, no. 10, pp. 3648—3653, October 2006.

Z. Liu and R.M. Weikle, II, “A high-order subharmonic mixer architecture using a phased local oscillator," IEEE Trans. Microwave Theory

and Tech., vol. MTT-54, no. 7, pp. 2977—2982, July 2006.

Z. Liu and R.M. Weikle, II, "A reflectometer calibration method resistant to waveguide flange misalignment," IEEE Trans. Microwave Theory and Tech., vol. MTT-54, no. 6, pp. 2447—2452, June 2006.

Z. Liu and R.M. Weikle, II, "A Compact Quadrature Coupler Based On Coupled Artificial Transmission Lines," IEEE Microwave and Wireless Components Lett., vol. 15, no. 12, pp. 889—891, December 2005.

T.W. Crowe, W.L. Bishop, D.W. Porterfield, J.L. Hesler and R.M.Weikle, II, "Opening the Terahertz Window with Integrated Diode Circuits," (invited) IEEE Journal of Solid-State Circuits, vol. 40, no. 10, pp. 2104—2110, Oct. 2005.

Z. Liu, J.C. Midkiff, H. Xu, T.W. Crowe, and R.M.Weikle, II, "Broadband 180° Phase-Shifters Using Integrated Submillimeter-Wave Schottky Diodes," IEEE Trans. Microwave Theory and Tech., vol. MTT-53, no. 9, pp. 2949—2955, Sept. 2005.

R.M. Weikle, II, T.W. Crowe, and E.L. Kollberg, "Multiplier and Harmonic Generator Technologies for Terahertz Applications," Internat. Journal of High Speed Electronics and Systems (World Scientific Publishing Co.), vol. 13, no. 2, 429—456, 2003.

Number of Papers published in peer-reviewed journals: 23.00

(b) Papers published in non-peer-reviewed journals or in conference proceedings (N/A for none)

Number of Papers published in non peer-reviewed journals: 0.00

(c) Presentations

Number of Presentations: 0.00

Non Peer-Reviewed Conference Proceeding publications (other than abstracts):

Number of Non Peer-Reviewed Conference Proceeding publications (other than abstracts): 0

Peer-Reviewed Conference Proceeding publications (other than abstracts):

X. Li, A. Bykhovski, B. Gelmont, T. Globus, D.Woolard, M. Bykhovskaia, “Computational Methods for Analysis of Terahertz Spectral Signatures of Nucleic Acids”, 5th IEEE Conference on Nanotechnology, Nagoya, Japan, July 11-15, 2005, IEEE PRESS BOOKS, vol. 1, 221 – 224 (2005).

A. Bykhovski, X. Li , T. Globus, T. Khromova , B. Gelmont , D. Woolard , A. C. Samuels, and J. O. Jensen, “THz absorption signature detection of genetic material of E. coli and B. subtilis”, SPIE Proceed. V 5995, pp.59950N-1:10, 2005, Optics East, Boston, Oct. 2005.

T. Globus, T. Khromova , B. Gelmont , D. Woolard , and L. K. Tamm, “Terahertz characterization of diluted DNA solutions”, Proceedings of SPIE Photonics West 2006 “Biomedical Vibrational Spectroscopy III: Advances in Research and Industry”, v. 6093, Biomedical Optics Symposium, San Jose, California, 21-26 January 2006.

T.Globus, T. Khromova, D. Woolard and A. Samuels, “THz Resonance Spectra of Bacillus Subtilis Cells and Spores in PE Pellets and Dilute Water Solutions,” SPIE Proc. V.6212-21, Defense and Security Symposium (DSS06); Conference: Terahertz for Military and Security Applications IV, Orlando, Florida, Apr.17-21, 2006.

T. Globus, T. Khromova , D. Woolard and A. Samuels, “THz Resonance Spectra of Bacillus Subtilis Cells and Spores in PE Pellets and Dilute Water Solutions”, SPIE Defense and Security Symposium, V 6212-21, Orlando, Florida, 17-21 April 2006.

A. Bykhovski, T. Globus, T. Khromova , B. Gelmont , D. Woolard , and M. Bykhovskaia , “An Analysis of the THz Frequency Signatures in the Cellular Components of Biological Agents”, SPIE Defense and Security Symposium 2006, V 6212-18, p. 132-141. Orlando, Florida, April 2006.

Analysis and Design of Terahertz Transit Time Diodes,” X. Bi,J. East, U. Ravaioli and G. Haddad, 16th International Conference on Space Terahertz Technology, May 2-4, 2005, Goteborg, Sweden.

“Remote Detection of Bioparticles in the THz Region,” E.R. Brown, D.L. Woolard , A. C. Samuels, T. Globus, and B. Gelmont, Proceedings of the International Microwave Symposium, Seattle, WA, 6 June 2002, p.1591-4 vol.3. 19

“Terahertz-Frequency Remote-Sensing of Biological Warfare Agents,” D.L. Woolard, E.R. Brown, A. Samuels, J. Jensen, T. Globus, B. Gelmont, and M. Wolski, 2003 IEEE MTT-S Digest (IEEE, New York, 2003).

“Toward the Remote Sensing of Bacterial Endospores by Raman Lidar,” A.W.M. Lee, E.R. Brown, F. Ow, and R. Garrell, Proc. 2003 Int. Symp. on Spectral Sensing Research.

“THz Signature Characterization of Bio-Simulants,” A. Majewski, P. Miller, R. Abreu, J. Grotts, T. Globus, and E.R. Brown, Proc. SPIE, vol. 5790, paper 9 (2005).

“A novel I-RTD based optically pulsed hybrid device for generating THz oscillations,” W. Zhang, D. L. Woolard, E.R. Brown, and B. Gelmont, Proc. of the SPIE, Volume 5995, pp. 245-256 (2005)

“An Optically-Triggered I-RTD Hybrid Device for Continuous-Wave Generation of THz Oscillations” D.L. Woolard, W. Zhang, E.R. Brown , B. Gelmont and R. Trew, Proc. SPIE, Volume 6212, pp. 621207 (2006).

D. Hui and R.M. Weikle, II, “Calibration of six-port reflectometers using null double injection," 67th ARFTG Microwave Measurement Conference Digest, San Francisco, CA, pp. 164—179, June 2006.

Z. Liu and R.M.Weikle, II, “A 180° Hybrid Based On Coupled Asymmetrical Artificial Transmission Lines," 2006 IEEE Int. Microwave Symposium Digest, San Francisco, CA, pp. 1555—1558, June 2006.

H. Xu, Z. Liu, C.H. Smith, III, J.L. Hesler, B.S. Deaver, Jr. and R.M. Weikle, II, “A Non-Contacting Tunable Waveguide Backshort for Terahertz Applications," 2006 IEEE Int. Microwave Symposium Digest, San Francisco, CA, pp. 1919—1922, June 2006.

L. Yang, T. Kotchiev, Z. Liu, and R.M. Weikle, II, “New calibration method for measuring permittivity of biological material with W-band waveguide," Proceedings of the Joint 31st International Conf. On Infrared And Millimeter Waves and the 14th International Conference On Terahertz Electronics, Shanghai, China, p. 408, September 2006.

R.M. Weikle, II, Z. Liu, L. Yang, S. Űlker, and A.W. Lichtenberger, “Sampled-Line Reflectometers for Terahertz s-Parameter Measurements," Proceedings of the SPIE, Conference 5790, Terahertz for Military and Security Applications III, Orlando, FL, pp.

137—148, March 2005.

R.M. Weikle, II, Z. Liu, Heng Liu, Lei Liu, S. Űlker, A.W. Lichtenberger, “Six-port reflectometers for terahertz scattering parameter measurements using submillimeter wavelength detectors," Proceedings of SPIE, Conference 5592 on Nano-Fabrication: Technologies, Devices and Applications, Philadelphia, PA, pp. 328—340, October 2004.

Z. Liu, J.C. Midkiff, and R.M. Weikle, II “Millimeter-Wave Phase Shifters Utilizing Planar Integrated Schottky Barrier Diodes," 2003 IEEE Int. Microwave Symposium Digest, Philadelphia, PA, pp. 2241—2244, June 2003.

H. Xu, J.L. Hesler, Y. Duan, T.W. Crowe, and R.M. Weikle, II “A Heterostructure Barrier Varactor Sideband Generator," 2003 IEEE Int. Microwave Symposium Digest, Philadelphia, PA, pp. 2031—2034, June 2003.

S. Űlker, R.M. Weikle, II, “Submillimeter-Wave Scattering Parameter Measurements With A Sampled-Line Six-Port Reflectometer," 60th ARFTG Conference Digest,Washington D.C., pp. 71—80, December 2002.

Number of Peer-Reviewed Conference Proceeding publications (other than abstracts): 22

(d) Manuscripts

“An Optically Triggered I-RTD Hybrid THz Oscillator Design,” D.L. Woolard, W. Zhang, E.R. Brown, B. Gelmond, and R. Trew, accepted to Int. J. High Speed Electronics and Systems, 2007.

Number of Manuscripts: 1.00

Number of Inventions:

Graduate Students

NAME	PERCENT_SUPPORTED	
Xiaowei Li	1.00	No
Ying Luo	0.50	No
Ramakrishnan Parthasarathy	0.50	No
Xichuan Bi	1.00	No
Zhiyaing Liu	0.50	No
Li Yang	1.00	No
Sad?k ?lker	1.00	No
Heng Liu	1.00	No
FTE Equivalent:	**6.50**	
Total Number:	**8**	

Names of Post Doctorates

NAME	PERCENT_SUPPORTED	
Zhiyang Liu	0.50	No
Sadik Ulker	1.00	No
FTE Equivalent:	**1.50**	
Total Number:	**2**	

Names of Faculty Supported

NAME	PERCENT_SUPPORTED	National Academy Member
Tatiana Globus	0.50	No
Boris Gelmont	0.50	No
Robert M. Weikle, II	0.15	No
Thomas W. Crowe	0.20	No
Jeffrey L. Hesler	0.30	No
Elliott Brown		No
Jack East		No
George I. Haddad		Yes
Neal Stewart		No
Hong-Liang Cui		No
Maria Bykhovskaia		No
FTE Equivalent:	**1.65**	
Total Number:	**11**	

Names of Under Graduate students supported

NAME	PERCENT_SUPPORTED	
Brian J. Cobb	0.25	No
FTE Equivalent:	**0.25**	
Total Number:	**1**	

Names of Personnel receiving masters degrees

NAME	
Heng Liu	No
Ramakrishnan Parasarathy	No
Total Number:	**2**

Names of personnel receiving PHDs

NAME	
Zhiyang Liu	No
Sadik Ulker	No
Xichuan Bi	No
Total Number:	**3**

Names of other research staff

NAME	PERCENT_SUPPORTED	
Alexei Bykhovski		No
Tatyana Khromova		No
FTE Equivalent:		
Total Number:	**2**	

Sub Contractors (DD882)

Inventions (DD882)

Final Progress Report

on

Science and Technology of Biological and Chemical Sensing at Terahertz Frequencies

Contract No. ARO-MURI-DAAD19-00-R-0010

To

U.S. Army Research Office

Attention: Dr. Dwight L. Woolard, Program Manager

February 28, 2007

Principal Investigator:

Robert M. Weikle, II
Associate Professor
Department of Electrical and Computer Engineering
University of Virginia
Charlottesville, VA 22903
(434) 924-3362

TABLE OF CONTENTS

Terahertz Wave Interaction with Biological Macromolecules
(Experiment and Simulation)

Objective:

To discover and understand the fundamental physical principles governing the interactions of biological molecules with electromagnetic radiation in the terahertz region of the spectrum. The *primary goals* are to observe the resonant modes in absorption spectra within the submillimeter wave range and to demonstrate the fundamental character of the submillimeter-wave spectral absorption, thereby, establishing a physical confirmation that very long wavelength resonant features result from electromagnetic wave interactions with the DNA and RNA macromolecules – phonon modes.

Impact of the Research:

The lead research component is focused on the molecular structure, dynamical properties, and the THz interaction mechanisms related to CBW agents in order to develop a scientific base for THz-frequency sensing. The impact of this research will be to establish the initial foundation for the future use of terahertz spectroscopy in the identification and characterization of biological macromolecules and related materials.

Technology Transfers and Research Collaborations:

This research results from collaboration with Dr. D. Woolard (ARO), Dr. A. Samuels and Dr. J. Jensen (Edgewood Chemical and Biological Center), with the group of Prof. T. Crowe (UVA and Virginia Diodes Inc.), groups of Prof. R. Weikle (UVA), Prof. Lucas Tamm (UVA), Prof E. Fernandez (UVA), Prof. D. Theodoresku and Prof. H. Frierson (UVA), the group of Prof. N. Stewart (the University of Tennessee), with the group of Prof. E. Brown (UCLA), Lowell University in Massachusetts, Goodrich Co. Results of characterization immediately transfer to Edgewood Chemical and Biological Center. Developed technology for fingerprinting of biological materials in the THz spectral range was used to construct a predicted database for THz signature of bio-warfare agents using experimental transmission spectroscopy and modeling in a DTRA/CBT Project "*New Concepts for Detection Biological Targets:* Terahertz Signature Data Base Generation",the proposal number: P-47213_EL-CDP, grant No: W911NF-05-1-0033 (***BAA05DET014: UVA,*** Task: ***47213-EL-CDP,*** Dr. Ngai M. Wong)**,** PI T. Globus**.** The results will be also used in future development of biosensing technology (Virginia Diodes).

Summary of Achievements:

- The fundamental physical nature of the observed resonance structures in THz spectra of biological macromolecules which is caused by the internal vibration modes in macromolecules was further confirmed and studied. The initial successful demonstration of these phenomena in solid films of DNA, RNA, short-chained oligonucleotides of known base-pair sequences and spores was extended to include proteins, cells and tissues and bio materials in liquid phase.

- Reflection of double- and single-stranded DNA from herring and salmon as well as samples of protein Ovalbumin and Bacillus Subtillus spores were measured and dielectric properties

of biological molecules in the Terahertz gap (refractive index and absorption coefficient spectra) were characterized.

- First measurements of BG cells in the form of aerosol were conducted using FT spectroscopy which demonstrated very high sensitivity for low material concentration. Results of characterization were transfer to the Goodrich Co for use in developing a system for remote sensing.

- Application of THz Spectroscopy for biomedical research: characterization of cancer cells and tissue.

- Characterization of Proteins to demonstrate the capability of THz FT spectroscopy of discriminating between different protein conformations and of monitoring the folding-unfolding process.

- Developing THz characterization technique for diluted solutions of biological materials for possible future applications in real time monitoring of biological processes on molecular level and detecting water contaminations.

- Further development of theoretical modeling: developing realistic modeling approach and application of Amber and other available packages to calculate the spectra of short- and macromolecules.

- The new THz characterization technique for diluted solutions of biological materials. developed a new technique for structural characterization of DNA, proteins and related materials in diluted solutions by taking advantages from lower liquid water absorption at the lower frequency end of THz vs. IR and far IR regions. Reduced the amount of biomaterial in one sample required for characterization or detection. The simple technique for liquid sample preparation was developed: samples with less than 10 ml of water solutions kept between two polyethylene (PE) or polycarbonate (PC) films ~10 mm thickness, with the concentration from 0.01 mg/ml or 0.001%. The amount of solution is controlled by the spacer with the thickness from 12 mm.

Scientific Personnel Supported by Project:

Faculty
Dr. Tatiana Globus
Dr. Boris Gelmont
Dr. Alexei Bykhovski
Dr. Maria Bykhovskaia
Dr. Tatyana Khromova

Graduate Research Assistants
Xiaowei Li
Ying Luo
Ramakrishnan Parthasarathy

Publication List :

- X. Li, A. Bykhovski, B. Gelmont, T. Globus, D.Woolard, M. Bykhovskaia, "Computational Methods for Analysis of Terahertz Spectral Signatures of Nucleic Acids", 5th IEEE Conference on Nanotechnology, Nagoya, Japan, July 11-15, 2005, IEEE PRESS BOOKS, vol. 1, 221 – 224 (2005).
- A. Bykhovski, X. Li , T. Globus, T. Khromova , B. Gelmont , D. Woolard , A. C. Samuels, and J. O. Jensen, "THz absorption signature detection of genetic material of *E. coli* and *B. subtilis*", SPIE Proceed. V 5995, pp.59950N-1:10, 2005, Optics East, Boston, Oct. 2005.
- R. Parthasarathy, T. Globus, T. Khromova, N. Swami, D. Woolard, "Dielectric properties of biological molecules in the Terahertz gap", J.Appl. Phys. Lett., v. 87, 11, 2005.
- T.Globus,D.Woolard,T.W.Crowe, T.Khromova, B. Gelmont, J. Hessler, "Terahertz Fourier transform characterization of biological materials in a liquid phase", J. Phys. D: Appl. Phys. 39 3405-3413 (2006).
- E.R. Brown,T.B. Khromova, T. Globus, D.L. Woolard, J.O. Jensen and A. Majewski, "THz-Regime Attenuation Signatures in *Bacillus subtilis* and a Model Based on Surface Polariton Effects", IEEE Sensors Journal, Febr. 2006.
- T. Globus, T. Khromova , B. Gelmont , D. Woolard , and L. K. Tamm, "Terahertz characterization of diluted DNA solutions", Proceedings of SPIE Photonics West 2006 "Biomedical Vibrational Spectroscopy III: Advances in Research and Industry", v. 6093, Biomedical Optics Symposium, San Jose, California, 21-26 January 2006.
- T.Globus, T. Khromova, D. Woolard and A. Samuels, "THz Resonance Spectra of Bacillus Subtilis Cells and Spores in PE Pellets and Dilute Water Solutions," SPIE Proc. V.6212-21, Defense and Security Symposium (DSS06); Conference: Terahertz for Military and Security Applications IV, Orlando, Florida, Apr.17-21, 2006.
- T. Globus, T. Khromova , D. Woolard and A. Samuels, "THz Resonance Spectra of Bacillus Subtilis Cells and Spores in PE Pellets and Dilute Water Solutions", SPIE Defense and Security Symposium, V 6212-21, Orlando, Florida, 17-21 April 2006.
- A. Bykhovski, T. Globus, T. Khromova , B. Gelmont , D. Woolard , and M. Bykhovskaia , "An Analysis of the THz Frequency Signatures in the Cellular Components of Biological Agents", SPIE Defense and Security Symposium 2006, V 6212-18, p. 132-141. Orlando, Florida, April 2006.
- D. L. Woolard, Y. Luo, B. L. Gelmont, T. Globus and J. O. Jensen, "Bio-molecular inspired electronic architectures for enhanced sensing of thz-frequency bio-signatures", International Journal of High Speed Electronics and Systems (IJHSES), Vol.20, No. 10, 1-15 (2005).

Conclusions :

- Demonstration of the fundamental character of resonance features in transmission (absorption) spectra of biological materials in the THz spectral range.

- These resonances arise from electromagnetic wave interactions with the low frequency vibrational modes within biological macromolecules involving the weakest hydrogen bonds and/or non-bonded interactions between different functional groups or even between molecules.

- THz transmission (absorption) spectroscopy of biological macromolecules can reveal these multiple resonances and the spectra can be used for detection and for characterization of bio-polymers.

- Demonstration that Fourier Transform spectroscopy can be used to measure low frequency vibrational modes of biomolecules in dilute water solutions at the THz frequencies 10-25 cm -1. Our results indicate the interaction between biological molecules and substrate material is significant and likely controlled by substrate surface charges. This interaction causes the first monolayer of biomolecules to adsorb to the substrate in specific orientations.

- Orientation effects contribute significantly to the resonant features in the THz spectra.

- The band around 14 cm^{-1} is very sensitive to the orientation of the DNA molecules and can be used as a key to control the preferable direction of material orientation.

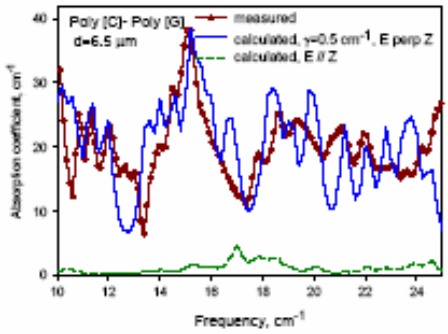

Direct comparison of experimental spectrum (red) with theoretical prediction (blue) for a short chain DNA fragment with known structure.

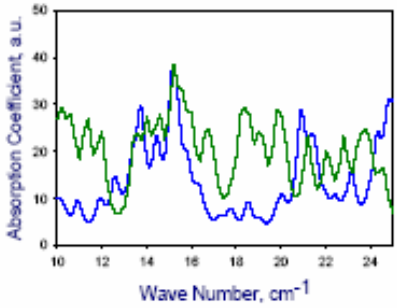

Simulation results using Jumna (green) and Amber (blue).

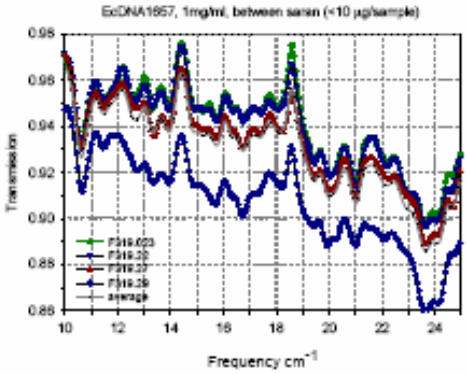

Good reproducibility of spectral features of a E. coli DNA sample (concentration 1 mg/ml or 0.1%) between two Saran films.

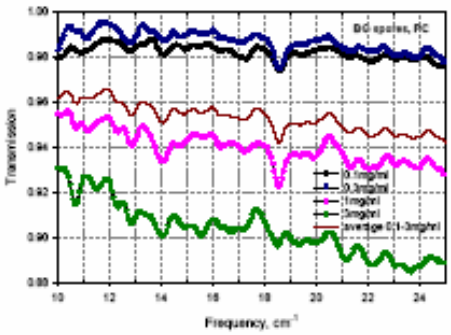

BG spores suspended in water between 2 PC substrates. Different concentrations and averaged.

Solid-State Transit Time THz Sources

X. Bi , J. East and G. Haddad
Solid State Electronics Laboratory
The University of Michigan

This report is a brief summary of the results of the project. The details of the research are described in a Ph.D. Thesis, "Analysis and Design of Si/SiGe Terahertz Diodes" by Xiaochuan Bi, a student that was supported by the project.

Summary:

The goal of the research in this project was to investigate novel THz sources. The effort started with an investigation of vacuum Thz transit time diodes. These devices overcome many of the limitations of semiconductor based transit time device oscillators. In particular the drift region dielectric constant is the vacuum value and the drift velocities are ballistic rather than scattering limited. The lower dielectric constant will lower the capacitance per unit area and the higher velocity associated with ballistic transport will increase the drift region length, further reducing the cold capacitance. This combination will allow a larger device area for a given impedance level and frequency, which should increase the power available from the device. The ballistic nature of the electron transport is also an advantage. In a conventional semiconductor based device the carrier velocity is near the saturated value and the resulting induced current is approximately rectangular. In the vacuum structure the acceleration rather than the velocity is nearly constant and the resulting induced current is triangular, improving the power generation in the second ½ of the RF cycle. Detailed numerical results indicated that this new device could produce useful power at Thz frequencies. However, we had major problems when we tried to fabricate experimental structures. The critical part of the experimental structure was the field emitter cathode. This cathode was based on a micromachined silicon structure that used nanoscale silicon tips as field emitters. Earlier research showed that these tip arrays could provide modest current densities. The earlier work was based on using the emitters for very low frequency display applications. However, although some of the experimental structures produced current densities high enough to be useful the experimental results were not reproduceable and possible improvements to the structure would introduce additional capacitance that would short out the RF portion of the transit time structure. Therefore, we decided to refocus the research on more conventional semiconductor based structures. These results will be described next.

Transit time sources have a long history but there are several reasons to revisit them for use as very high frequency sources. Early devices were based on silicon technology but recent research has focused on III-V materials, partly because of the use of MBE to realize very precise doping profile control. However improvements in silicon MBE associated with improvements in SiGe HBT's overcomes this disadvantage. The material properties of the III-V devices were better for microwave frequencies. However, these advantages can become limitations at THz frequencies. Finally, at higher frequencies a more detailed physical model is needed to describe the transport. An electron traveling at a velocity of 10^7cm/sec in an electric field of 1 MV/cm will gain 1 eV of energy in 10 nanometers and 0.1 psec. These distance and time scales can be neglected at microwave

and millimeter wave frequencies but become important approaching THz frequencies. A major portion of the effort in the project involved a detailed transport level investigation of the limitations of THz transit time devices.

The research implemented a Monte Carlo simulation of Si and SiGe transit time devices. The results showed two important transport effects that are not accurately described by simpler techniques. The first is velocity overshoot. Velocity overshoot improves the performance of most transistors but degrades transit time device operation by increasing the induced current near the injection phase. The design goal becomes to reduce the transient overshoot as much as possible. This means that silicon with a modest velocity overshoot is a better choice for THz transit time devices than III-V materials. Overshoot can also be reduced by injecting carriers at a higher energy. This means that higher injection energies after ionization is better than lower injection energies after tunneling injection. Both of these results are new.

The second important transport effect is energy conservation or "dead zones". At lower frequencies the generation region can be defined with a high field using the doping profile. However, in higher frequency devices the voltages are lower and the ability to define the generation region with the doping profile is reduced as the generation spills into the drift portion of the device. Finally for very short structures the generation extends over most of the device. Again a Monte Carlo analysis that includes energy conservation effects is needed to accurately model device performance. A detailed analysis of silicon devices operating between 200 and 500 GHz was carried out using the Monte Carlo simulation. It was clear that generation region design limitations associated with energy conservation were the fundamental limit on extending the high frequency operation. At this point we investigated an alternative generation region design, a SiGe heterostructure. This design will have a lower ionization rate material between two higher ionization Si drift regions. This structure will have a better carrier generation confinement and better induced current waveform. A variety of SiGe based structures were analyzed to optimize the operation above 200 GHz. The large-signal results showed that the SiGe MITATT diode improves the power generation by 63% at 200 GHz and 20% at 250 GHz. For frequencies beyond 300 GHz, both Si and SiGe MITATT diodes showed great promise for power generation. They produce more than 8 mW at 300 GHz and more than 1 mW at 400 GHz.

List of Publications Resulting from This Work:

"Analysis and Design of Si Terahertz Transit Time Devices", X. Bi, J. East U. Ravaioli and G. Haddad, Solid State Electronics, Issue 5, May 2006, pages 889-896.

"Analysis and Design of Terahertz Transit Time Diodes," X. Bi,J. East, U. Ravaioli and G. Haddad, 16th International Conference on Space Terahertz Technology, May 2-4, 2005, Goteborg, Sweden.

"Analysis and Design of Si/SiGe Terahertz Diodes", Xichuan Bi, Ph.D. thesis, The University of Michigan, 2007.

Scientific Personnel Supported by this Project:

Xichuan Bi, Ph.D.
Dr. Jack East, research scientist
Professor George Haddad, project director.

Science and Technology of Chemical and Biological Sensing at THz Frequencies

Final Report Contribution
Principal Investigator: E.R. Brown, Ph.D.
University of California, Santa Barbara 93106

Summary

Three highlight areas were chosen so summarize the research findings made by the group of E.R. Brown, first at UCLA between 2001 and 2004 and then at UCSB between 2004 and 2006. These are: (1) the development of the photomixing coherent transceiver and its application to THz spectroscopy, (2) high-resolution detection and modeling of spores of Bacillus subtilis, and (3) detection of surprisingly narrow THz absorption resonances in polysaccharides, particularly lactose monohydrate.

I. THz Photomixer Coherent Transceiver

A spectrometer needs both a source to illuminate a sample material of interest and a detector which measures how much gets through the sample. In this project we used two ErAs:GaAs photoconductive mixers for the source and detector (Fig. 1). The system is driven by two NIR lasers which makes it highly coherent (coherence bandwidth is <20 MHz), and therefore capable of measuring extremely narrow spectral features. It is tunable from DC to 3 THz within seconds. The two laser beams are offset in wavelength and mixed together in a biased photoconductors to generate a cw THz beam at the lasers' difference frequency. This is similar to difference frequency generation in nonlinear crystals but since bias is applied to the photoconductor, the mixing gains power from the applied bias. Also, since the mixing occurs within a short length in the semiconductor it eliminates the requirement for phase matching. Due to the reciprocity theory in electromagnetics, the role of the bias and the THz beam in a photomixer in interchangeable. This can be seen in Fig 1., where the transmitting photomixer, generates THz power when biased, whereas the receiver (Rx) on the right side, generates current when THz power is incident. Ultrafast, low-temperature-grown (LTG) GaAs photoconductors are now commonly used for making short broadband pulses in switches for time domain spectroscopy systems (TDS) but in this system we use a superior ErAs:GaAs material system by collaboration with the material science department at UCSB. The advantage of the transceiver is that one can get the amplitude as well as the phase response of the material. To get information about the phase change in the system, a retromirror is moved to change the optical path on the transmitting photomixer by a few THz wavelengths. This renders a sinusoidal interferogram. With sufficient signal strength, the frequency, phase and amplitude of the wave can be determined. However, since the frequency can be easily determined with NIR analysis of the pump laser beams, this can be used to create a matched filter that correlates the sinusoidal interferogram with the interferogram to be expected. This enables phase and amplitude determination even when the noise is larger than the signal.

Fig. 2 shows the spectral response if the transceiver during a fast scan with broad frequency coverage. The maximum current in the receiver is 5 nA when the THz power is approximately 10 microwatts. The static ($I_{Rx}/P_{opt}^{1/2}$) and differential sensitivities (dI_{Rx}/dP_{opt}) are 20μA/W$^{1/2}$ and 40 mA/W respectively. As a spectroscopically qualitative

test for the performance of the transceiver system, the transmission through air between 1.2 and 1.8 THz was measured as shown in Fig 3. This frequency region was chosen because it contains well understood water vapour absorption lines. At each frequency data point, the interferogram was measured while dithering a retro-mirror by 2 cm over a 10s period at each frequency point. Fig. 3 shows that the amplitude data (blue dots) agree very well with theoretical model based on HITRAN parameters (solid black line), both in frequency location and intensity. The ratio maximum signal measured to the minimum is over 50dB. On the right side figure the change in index of refraction of the air in the path (blue dots) is plotted along with theory (solid red line). This shows that the system is successfully acquiring the phase, tracking even rapid changes, almost discontinuities in the index of refraction.

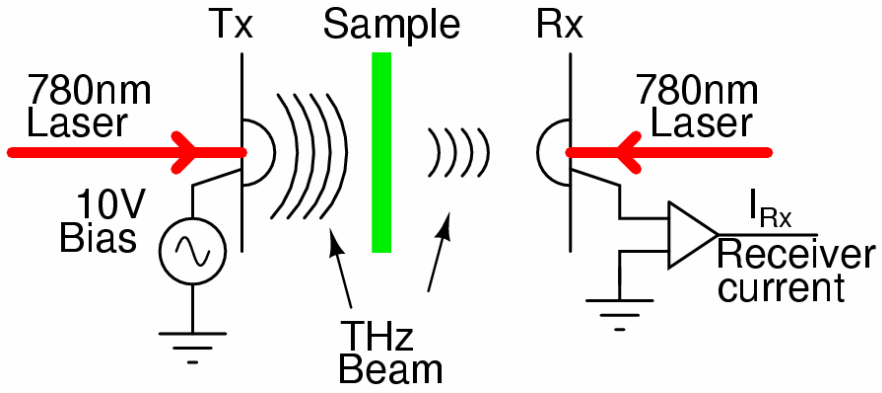

FIG. 1. Experimental setup. The THz beam is generated by transmitter (Tx), penetrates sample and is converted to current on the receiver (Rx).

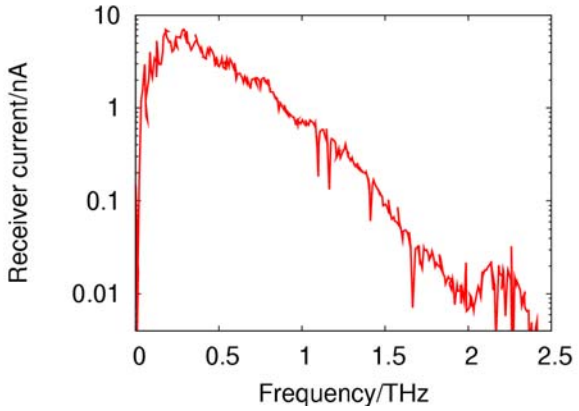

FIG. 2. Spectral response of coherent transceiver.

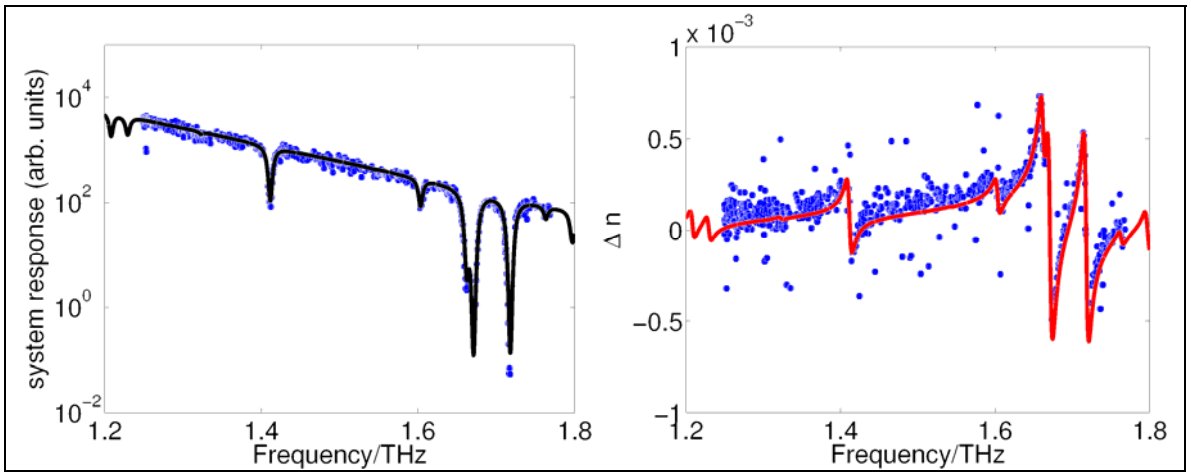

Fig 3. Amplitude (left) and phase (right) response of transceiver when scanning across atmospheric water vapor lines. The solid line is a Lorentzian model based on parameters from the HITRAN database.

II. Measurement and Modeling of Narrow Resonances in Bacillus Subtilis

Much of our research during the MURI concentrated on bioparticles, especially bacterial spores of the genus Bacillus. Scanning electron microphotographs (SEMs) of a typical spore of B. subtilis var. niger (formerly known as Bacillus globigii), or BG for short, indicate that it has a spheroidal shape with a length of ≈ 1.2 μm and width of ≈ 0.8 μm.[i] The spore outer coat (OC) represents approximately 30 to 60% of the dry weight of the spore. The OC is a tough proteinaceous layer having an unusually high content of cysteine and other hydrophobic amino acids. This makes the OC highly resistant to protein solvents, and also contributes to its rather high atomic density and dark appearance in SEMs. Also important to the present experiments is the reported crystallinity of this layer. As in other solids, crystallinity tends to support collective excitations, such as the phonons, and renders them with much longer lifetime than occurs in polycrystalline or ceramic materials.

In the MURI research samples of BG were prepared using spores mixed with vegetative-cell material and packaged in three different forms: (1) BG material only (vegetative cell matter plus spores), (2) BG material distributed in polyethylene (PE) powder, and (3) BG material suspended in air as an aerosol (done at the University of Virginia, Dr. T. Globus). The most important data was obtained on the diluted BG sample. Estimates of the mass fraction of this sample and the two others are listed in Table I. Optical microscopic inspection of the BG material showed that the vegetative-cell material were primarily in the form of pieces of broken cell-wall remnants.

For the purpose of extracting attenuation signatures, the desired quantity from the measurements was the transmission spectrum through each BG sample normalized to the transmission spectrum through its control sample. In principle, such normalization eliminates the effects of frequency-dependent source power, sample-dependent reflection coefficient, etc. The normalized transmission T'(ν) through the dilute-BG sample is plotted in Fig. 4 between 200 GHz and just under 1.08 THz, above which water vapor absorption reduced the SNR to unacceptable levels. The frequency registration and

normalization procedure does a good job of canceling the water absorption, but small undulations in T'(ν) still occur across the spectrum. These are attributable at least in part to small changes in the instrumental standing wave pattern caused by the changing of samples and the slight difference in their placement and refractive index. Provided that the refractive index and position is not changing with frequency, this type of undulation is expected to lie inside of an envelope defined roughly by the two dashed curves in Fig. 4. The vertical range of the envelope is ≈0.8 dB (17%)

Three attenuation signatures fall ~10% below the lower extent of the envelope as highlighted by the dotted rectangles. They are centered around 250, 415, and 1035 GHz, respectively, are progressively strong in attenuation, and have all been reported by other researchers, particularly Dr. T. Globus of U. Virginia. The first two signatures are regarded as probable detections since they correspond to the 275 and 425 GHz signatures of the concentrated-BG sample. The 1.035 THz signature is regarded as the most significant since it is stronger than the other two and has also been measured recently by time-domain THz spectroscopy.[ii] Again, ΔT' is derived by dividing out the broadband attenuation, this time taken as an average through to the center of the envelope. The corresponding spore concentration and attenuation cross section are listed in Table I. In comparing the dilute and concentrated-BG results, it is remarkable that 10 times *less* BG material (by mass) is producing 3 times *stronger* attenuation *per spore*. The linewidths are difficult to determine precisely, so are merely bounded in Table 1 as < 15 GHz (250 GHz signature) and < 10 GHz (415 GHz signature). They are somewhat narrower than the corresponding linewidths in the concentrated sample.

Additional work done under the MURI developed a physical model for the origin of the signatures observed in BG spores. The model is based on the existence of polar transverse optical (TO) phonons in the polycrystalline outer coat (OC) of each BG spore. The interaction of these TO phonons with THz radiation was analyzed by invoking conservation of energy and momentum, leading to a strong coupling effect between them called a *polariton*. The resulting dispersion relation, ω_S vs K (K being the *polariton* wave vector in the bioparticle), is typical of coupled-mode systems having two branches, and is shown for our BG spore model in Fig. 5(a). Strong coupling occurs only in and around the "gap" between the branches, the lower extent being ω_t, and the upper extent being $\approx[(\omega_t)^2 + (\omega_p)^2]^{1/2}$. An important aspect of the polaritonic coupling is the small size of the gap compared to the ω_t. This is caused by the small value of ω_p or, equivalently, the large mass of the unit cell. This has one important consequence on the THz optics: *the range of possible polariton frequencies associated with a particular TO-phonon resonance is very small.*

The overall effect on the propagating THz radiation occurs through the dielectric function which for polaritons and other harmonic-oscillator-like excitations in solids is often approximated in a first analysis by the Lorentzian expression

$$\varepsilon(\omega) = \varepsilon_0 + \frac{\omega_p^2}{\omega_t^2 - \omega^2 - j\gamma\omega}$$

where ε_0 is the background dielectric constant in the limit of high frequencies (>> ω_t), γ is the damping rate, $\omega_P = (\rho_C q^2/M)^{1/2}$ is the effective plasma frequency, q is the effective charge (and thus the degree of polarity), M is the mass per primitive unit cell, and ρ_C is the density of unit cells and hence of TO phonons. In bulk solids this would suffice in calculating the THz

attenuation properties. But in the present samples we must also account for the *particulate* nature of the BG spores, which is greatly facilitated by three facts. The first is that the spore size is ~300 times less than the radiative wavelengths of interest in the sub-THz region. This allows us to evaluate the electromagnetic interaction in the "electrostatic" limit whereby the exciting and scattered electric fields (**E**) are assumed to be spatially uniform around the particle. The second fact is that the spore shape is spheroidal, which from electrostatics makes the polarization field induced in the spore *uniform*.[iii] The third fact is that the spores in our dilute and aerosol samples are rarefied enough that they can be treated as independent scatterers. The spores then contribute to a radiative extinction coefficient, A, simply by $A = \rho_V C_A$ where ρ_V is their volumetric density and C_A is the absorption cross section plotted vs frequency in Fig. 5(b). Further details of the model can be found in the paper: "THz Regime Attenuation Signatures in Bacillus subtilis and a Model Based on Surface Polariton Effects," E.R. Brown et al, IEEE Sensors J., Vol. 6, No. 5, pp. 1076-1083 (2006).

Table I.

Spectral Feature [GHz]	BG Sample	Estimated Spore Density [cm^{-3}]	$\Delta T'^{*}$	C_A^{**} [cm^2]	$\Delta\nu$ [GHz]
~260	concentrated	$\sim 7\times10^{8}$	0.40	2.2×10^{-11}	20
	dilute	$\sim 7\times10^{7}$	0.75	6.8×10^{-11}	< 15
~420	concentrated	$\sim 7\times10^{8}$	0.30	2.9×10^{-11}	≈ 10
	dilute	$\sim 7\times10^{7}$	0.70	8.5×10^{-11}	< 10

* measured at minimum transmission of resonant signature
**estimated attenuation cross section *per spore*.

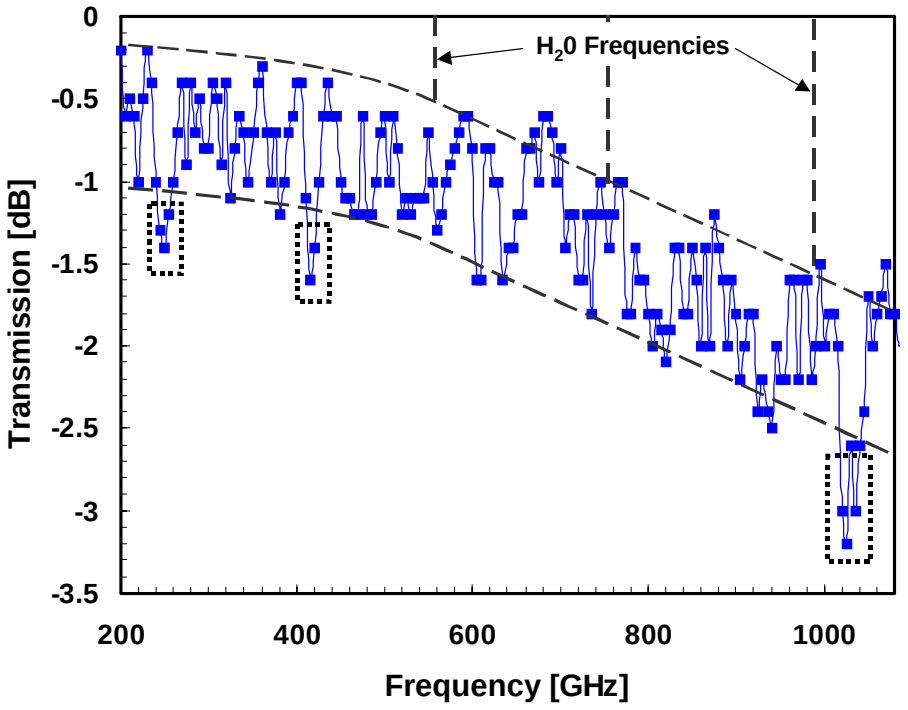

Fig. 4.

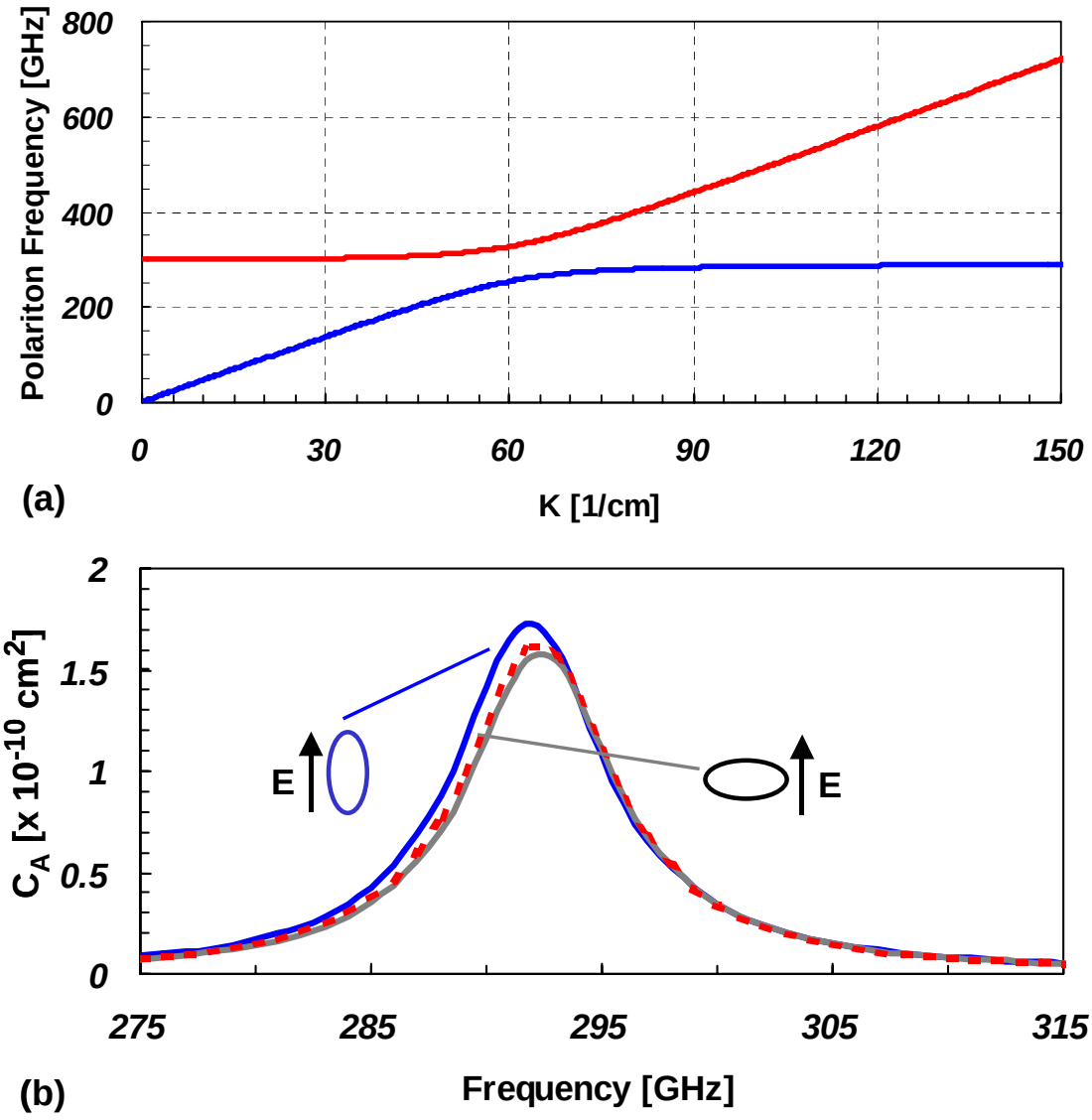

Fig. 5.

Polysaccharides

Most of the biomass on the planet consists of saccharides. Understanding their THz dynamics should therefore be of high significance to bimolecular detection. IR spectroscopy is used to examine the vibrational absorption spectrum of organic molecules. The frequency of these transitions is related to the strength of the chemical bond and mass of the bonded atoms. At lower frequencies, and specifically in the THz regime, one expects rotational spectral features or vibrational spectra of weaker bonds and larger masses. Polysaccharides have attracted attention in THz spectroscopy because they consist of hydrogen bonded networks of sugar molecules, saccharides. Each sugar

molecule is composed of two or more monosaccharides bonded together with an oxygen molecule. This gives rise to a large degree of freedom for oscillation within the sugar molecule.

One of the interesting things about sugars is that a very large family of anomers has exactly the same chemical composition but the alignment of chemical bonds makes the molecular dynamics and the biological role completely different. Because of the scale of the molecules THz spectroscopy is contains the ideal frequency range to directly detect the molecular dynamics and by comparing the spectra of different sugars.
We measured an absorption line in lactose around 518 GHz with a photomixing source and a room temperature bolometer as a detector. The samples were prepared by mixing 10% lactose and 90% polyethylene powder (PE) in a 10mm thick pellet. The spectrum is shown in Fig. 6. The line shape is fitted with a Lorentzian peak:

$$L(\upsilon) = \frac{J}{\pi}\frac{D}{D^2 + (\upsilon - \upsilon_0)^2}$$

And the fitting parameters for the half-width, D, were 16 GHz, the total intensity, A was 0.112 and the center was at 533 GHz. Fig. 6 also shows a spectrum taken without sample in the path and the residual error in the Lorentzian fitting. The linewidth of sub-THz absorption features (generally from lattice vibrations) in solids is excepted to inversely proportional to the scattering time of optical phonons. The line width of absorption features might thus have implications on the solid-state physics of the material, in particular, the interaction of phonons and the phonon density of states. In this case, the life time of this transition is $1/(2\pi \cdot 16\text{GHz}) \sim 70$ ps.

Fig. 7 shows the extraction of three absorption lines in Maltose monohydrate using a Lorentzian fit and assuming a Mie scattering background trend. Mie scattering is often seen in infrared spectroscopy of aerosol sub-wavelength particles. In our case we have higher dielectric powdered saccharides in a lower dielectric polyethylene powder matrix which has similarly Mie behaviour. The three Lorentzian peaks that were numerically extracted in maltose were located at: 1074, 1593, and 1985 GHz.
The contrast between these two samples, lactose and maltose which have the same composition, but completely different THz spectra, demonstrate how rich the THz spectra are in information about molecular structure beyond the composition.

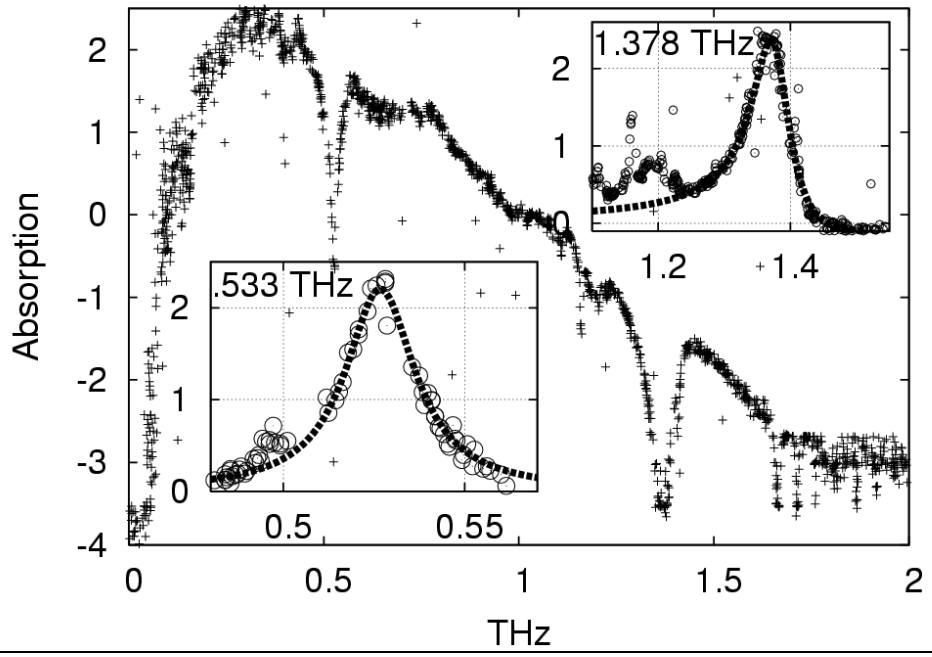

Fig. 6 Absorption in α-lactose monohydrate. The main graph shows the power spectrum of a photomixer illuminating a cryogenic bolometer with a lactose sample in between. The two insets show a fit to theoretical Lorentzian functions at 0.533THz and 1.378 THz. There is also possibly an absorption feature right below 1.2THz.

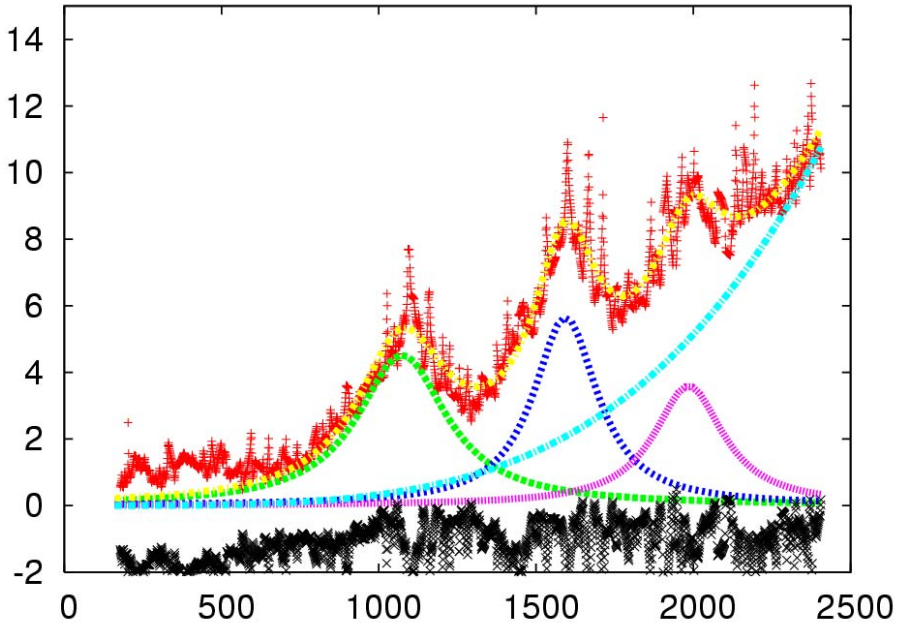

Fig. 7 Absorption in maltose monohydrate. The absorption spectrum of powdered maltose can be separated into a superposition of three Lorentzian absorption lines (1074, 1593, and 1985 GHz) and a Mie scattering background trend (λ^{-4}).

Book Chapters

"Fundamentals of Terrestrial Millimeter-Wave and THz Remote Sensing," E.R. Brown, in *Terahertz Sensing Technology*, Vol. 2: Emerging Scientific Applications and Novel Device Concepts, ed. by D.L. Woolard , W. R Loerop, and M.S. Shur (World Scientific, Singapore, 2004).

"Terahertz Generation by Photomixing in Ultrafast Photoconductors," E.R. Brown, in *Terahertz Sensing Technology*, Vol. 1: Electronic Devices and Advanced Systems Technology, ed. by D.L. Woolard , W. R Loerop, and M.S. Shur (World Scientific, Singapore, 2003).

Publications in Peer-Reviewed Journals

- "Optical Attenuation Signatures of Bacillus Subtilis in the THz Region," E.R. Brown, J.E. Bjarnason, T.L.J. Chan, A.W.M. Lee, and M.A. Celis, Appl. Phys. Lett., vol. 84 (no 18), p 3438-3440.
- "Millimeter-wave, terahertz, and mid-infrared transmission through common clothing" , J. E. Bjarnason, T. L. J. Chan, A. W. M. Lee, M. A. Celis, and E. R. Brown, Appl. Phys. Lett. vol. 85 (no. 4), pp. 519-521. [2004]
- "Attenuation contrast between biomolecular and inorganic materials at terahertz frequencies, T. L. J. Chan, J. E. Bjarnason, A. W. M. Lee, M. A. Celis, and E. R. Brown., Appl. Phys. Lett., vol. 85 (no. 13), pp. 2523-2525.. [2004]
- "ErAs:GaAs photomixer with two-decade tunability and 12 μW peak output power," J. E. Bjarnason, T. L. J. Chan, A. W. M. Lee, E. R. Brown, D. C. Driscoll, M. Hanson, A. C. Gossard, and R. E. Muller, Appl. Phys. Lett. , vol. 85 (no 18), p. 3983 [2004].
- "Room temperature, THz photomixing sweep oscillator and its application to spectroscopic transmission through organic materials", E. R. Brown, J. Bjarnason, T. L. J. Chan, D. C. Driscoll, M. Hanson, and A. C. Gossard, Rev. Sci. Inst., vol. 75 (no. 12) p. 5333 [2004]
- "Bright MM-Wave and THz Luminescence by Down-Conversion of near-IR Amplified-Spontaneous-Emission," E.R. Brown, J. E. Bjarnason, T.L.J. Chan, D. C. Driscoll, M. Hanson, and A.C. Gossard, Int. J. Infrared and MM Waves, Vol. 26, No. 12, pp. 1691-1702 (2005)
- "Terahetz Frequency Sensing and Imaging: A Time of Reckoning Future Applications," D.L. Woolard, E.R. Brown, M. Pepper, and M. Kemp, "Proc. IEEE, vol 93, (no 10), Oct. 2005.
- "Sensitivity measurement and analysis of an ErAs:GaAs coherent photomixing transceiver," J.E. Bjarnason and E.R. Brown, Appl. Phys. Lett., Vol. 87, 134105 (2005).
- "THz Regime Attenuation Signatures in Bacillus subtilis and a Model Based on Surface Polariton Effects," E.R. Brown, T.B. Khromova, T. Globus, D.L. Woolard, J.O. Jensen, and A. Majewski, IEEE Sensors J., Vol. 6, No. 5, pp. 1076-1083 (2006).
- "0.15-3.72 THz absorption of aqueous salts and saline solutions," J. Xu, K. W. Plaxco, S. J. Allen" J. E. Bjarnason, E. R. Brown, Appl. Phys. Lett, 90, 031908 (2007).
- "On the Strong and Narrow Absorption Signature in Lactose at 0.53 THz," E.R. Brown, J.E. Bjarnason, A.M. Fedor, and T.M. Korter Appl. Phys. Lett., vol. 90 061908 (2007).

Conference Papers and Proceedings

- "Remote Detection of Bioparticles in the THz Region," E.R. Brown**,** D.L. Woolard**,** A. C. Samuels, T. Globus, and B. Gelmont, Proceedings of the International Microwave Symposium, Seattle, WA, 6 June 2002, p.1591-4 vol.3.

- "Terahertz-Frequency Remote-Sensing of Biological Warfare Agents," D.L. Woolard, E.R. Brown, A. Samuels, J. Jensen, T. Globus, B. Gelmont, and M. Wolski, 2003 IEEE MTT-S Digest (IEEE, New York, 2003).
- "Toward the Remote Sensing of Bacterial Endospores by Raman Lidar," A.W.M. Lee, E.R. Brown, F. Ow, and R. Garrell, Proc. 2003 Int. Symp. on Spectral Sensing Research.
- "THz Signature Characterization of Bio-Simulants," A. Majewski, P. Miller, R. Abreu, J. Grotts, T. Globus, and E.R. Brown, Proc. SPIE, vol. 5790, paper 9 (2005).
- "A novel I-RTD based optically pulsed hybrid device for generating THz oscillations," W. Zhang, D. L. Woolard, E.R. Brown, and B. Gelmont, Proc. of the SPIE, Volume 5995, pp. 245-256 (2005)
- "An Optically-Triggered I-RTD Hybrid Device for Continuous-Wave Generation of THz Oscillations" D.L. Woolard, W. Zhang, E.R. Brown , B. Gelmont and R. Trew, Proc. SPIE, Volume 6212, pp. 621207 (2006).

Papers Submitted but not yet Accepted

- "An Optically Triggered I-RTD Hybrid THz Oscillator Design," D.L. Woolard, W. Zhang, E.R. Brown, B. Gelmond, and R. Trew, accepted to Int. J. High Speed Electronics and Systems, 2007.

Six-Port Reflectometers and Calibration Techniques for Submillimeter Measurement of Biological Materials

Summary

The test and measurement infrastructure that has been indispensable to the development and characterization of RF, microwave, and optical systems does not exist for the submillimeter-wave region of the spectrum. This has long been recognized as a major impediment to both the use and development of this spectral region and has impeded progress on the measurement and characterization of materials, including chemical and biological agents. This research effort is focused on the development of instrumentation, specifically, six-port reflectometers, to allow direct measurement of complex scattering parameters (magnitude and phase) of samples under test.

WAVEGUIDE-BASED REFLECTOMETERS

The most common transmission media in the submillimeter region are rectangular waveguide and free-space. Consequently, the reflectometers investigated under support of this MURI were designed using rectangular waveguide as the medium. The primary focus was on frequency bands extending beyond those currently covered by commercial equipment (300 GHz and higher). A photograph and detail of the prototype reflectometer developed under this grant is shown in Fig. 8. The instrument consists of a 5 cm section of rectangular waveguide and a set of four Schottky detector diodes. Because only three detectors are required to measure passive loads, three diodes serve as the primary detectors and the fourth is used as a backup. The diodes used in this work are SC1T5 planar Schottky diodes that were fabricated in the Microfabrication Laboratory at the University of Virginia. These devices are typically used for submillimeter-wave mixers operating near 600 GHz and have series resistance in the range of 6—9 Ω. Details of the waveguide and probe design are provided below:

Waveguide Design

The waveguide block used for this work was fabricated by Custom Microwave, Inc. The primary waveguide channel has dimensions of 406 μm X 787 μm, resulting in single mode propagation over the 190 GHz to 370 GHz band. Shallow (125 μm deep X 178 μm wide) cross channels are machined into the block to accommodate the microstrip probes that sample the standing wave in the guide. The dimensions of the cross channels were chosen to suppress excitation of high-order modes, leaving only the quasi-TEM shielded microstrip mode to travel to the diode detectors. The probe spacing is 195 μm, corresponding to $\lambda g/6$ at 320 GHz. Moreover, two narrow (100 μm wide) side channels are machined parallel to the primary waveguide channel (see Fig. 8(b)). These side channels allow quarter-wave long bond wires to be included as dc returns-to-ground for the Schottky power detectors. The waveguide flanges are designed to mate with standard WR-3 components.

Probe Design and Assembly

Sampling probes and microstrip lowpass filters for the reflectometer were designed with the use of Ansoft's *High Frequency Structure Simulator* (HFSS). To minimize perturbations to the standing wave in the guide and loading by the detectors, the probes were originally designed to couple a maximum of 5% of the incident power in the guide to the detectors. A second set of probes were also designed to increase the coupling to 15%. The probes and filters were fabricated using standard photolithographic techniques on 125 μm thick quartz substrates. Low-pass filter sections integrated with the probes were designed to block the 270—320 GHz submillimeter

signal while permitting dc biasing of the detectors. Corrections for step discontinuities and the effect of the waveguide cover shielding the microstrip structure were analyzed and compensated for with the aid of HFSS. The low-pass filter consists of an 10-section stepped impedance line with low impedance sections of 65Ω and high impedance sections of 145Ω.

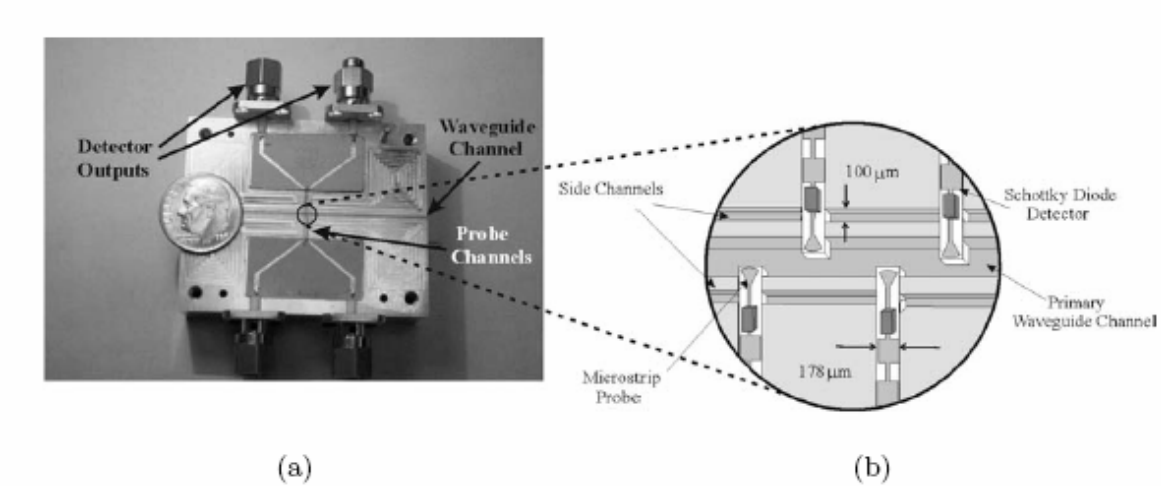

Fig. 8. (a) Photograph of the submillimeter sampled-line reflectometer. (b) Detail showing the waveguide dimensions and placement of the sampling probes.

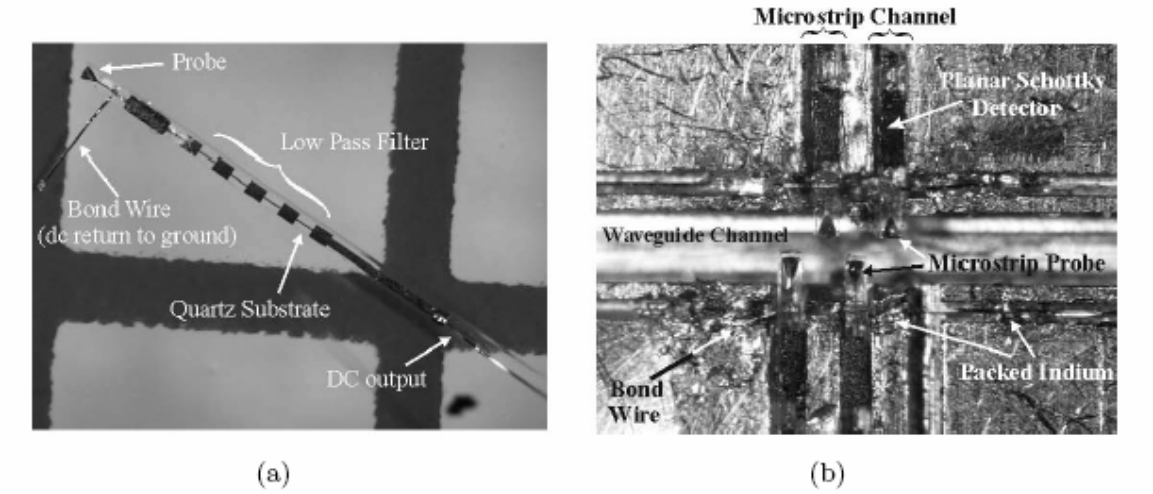

Fig. 9. (a) Photograph of a completed detector circuit showing the flip-chip mounted diode, waveguide probe, low-pass filter, and dc return-to-ground. (b) Photograph of the reflectometer showing the positions of all four sampling probes.

100 μm wide gaps included in the probe design accommodate the detectors. Small amounts of silver epoxy are applied on either side of these gaps and the diodes are flip-chip mounted across the gaps. The epoxy is then cured in a temperature controlled oven at 100 C for approximately two hours. The final step in assembly consists of mounting the probes to their respective locations in the block. This is done using commercially available UV-cured epoxy. A photograph of a completed probe circuit is shown in Fig 9(a) and the completed reflectometer is shown in fig 9(b)

Measurements and Characterization

The experimental setup used to evaluate the sampled-line re°ectometer is shown in fig. 10. A commercial frequency synthesizer (model HP-8350B, 50 MHz—22 GHz) is used as the primary source. This is followed by a broadband frequency tripler (model 295-320FEM) designed and fabricated by Virginia Diodes, Inc. An adjustable attenuator placed before the tripler permits control of the input power provided to the reflectometer. DC bias is supplied to the Schottky detectors with commercial bias supplies (model E3610A by Hewlett Packard) and the output current of the detectors is monitored with a set of Keithley-2000 6 – 1/2 digit multimeters

To establish that the sliding termination used to calibrate the sampled-line reflectometer behaves as desired, the power detected by the Schottky diodes was measured as a function of backshort position. Figure 11(a) shows the measured current through one of the detectors as a function of backshort position. For this measurement the input submillimeter-signal was fixed at 300 GHz. In addition to allowing the performance of the backshort to be assessed, the measurement shown in fig. 11(a) shows there is no significant harmonic content in the source signal other than the fundamental. Because the six-port method relies on direct detection, it can be susceptible to spurious responses arising from the presence of harmonics. Figure 11(b) shows the measured locus the sliding short traces out in the reflection coefficient (Γ) plane at 300 GHz. This measurement was done using the sampled-line reflectometer after it had been fully calibrated. For comparison, the locus produced by the sliding load was also measured using an HP8510C vector network analyzer outfitted with the Oleson Microwave Laboratory's (OML) V03VNA-T/RX2 module (shown in figure 11(b)).

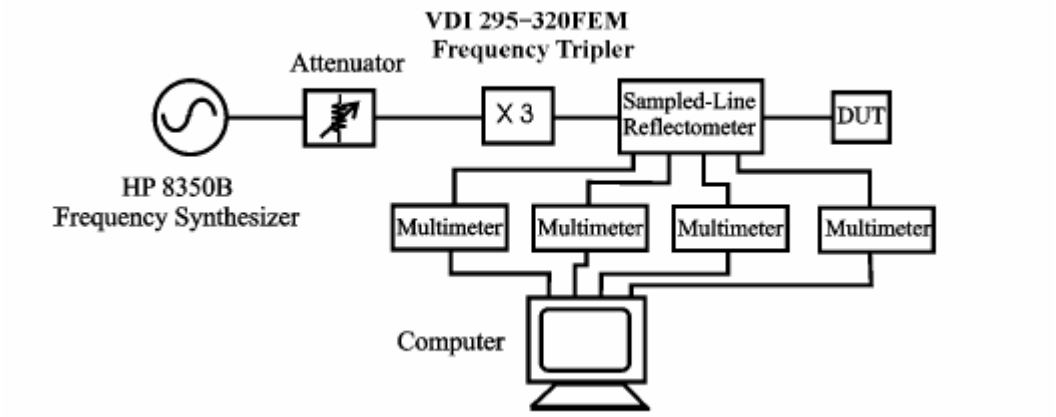

Fig. 10. Experimental setup for testing and evaluating the sampled-line reflectometer.

The second calibration step for the reflectometer consists of using three well-characterized standards to determine the complex coefficients for the standard one-port error model. In this work, the custom-made short circuit and two offset shorts previously described were used for this calibration step.

Initial measurements performed on the system utlized the probes with low coupling (5%). Above 300 GHz, two of the diode detectors exhibited very low responsivities, near the noise floor of our measurement system. It is believed that this behavior is likely a result of misalignment and inaccurate placement of the diode chips/probes associated with the manual assembly of the reflectometer. As a result, scattering parameter measurements in the 270 GHz to 300 GHz range are presented. Verification standards are not available for the submillimeter-wave range. Consequently, operation of the reflectometer was evaluated using the offset shorts designed for

calibration. Because only two offset shorts (of lengths 33 mils and 37 mils) are used in the calibration procedure for the 270 GHz to 300 GHz range, a third offset (70 mils) can be used as a check to verify the reflectometer is functioning properly. Remeasurement of the standards used for calibration provides additional information regarding the repeatability of measurements.

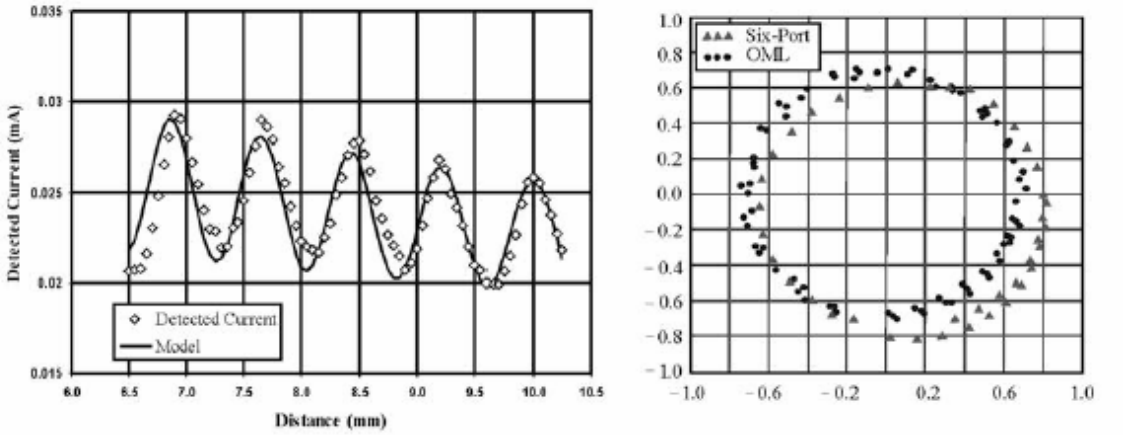

Fig. 11. (a) Plot of the detected current vs. position for the sliding load used to calibrate the reflectometer. For this measurement, the submillimeter source was set to 270 GHz and a single diode detector was used. (b) Loci traced out by the sliding short in the Γ-plane measured with the sampled-line reflectometer and the commercially available OML V03VNA-T/RX2 module

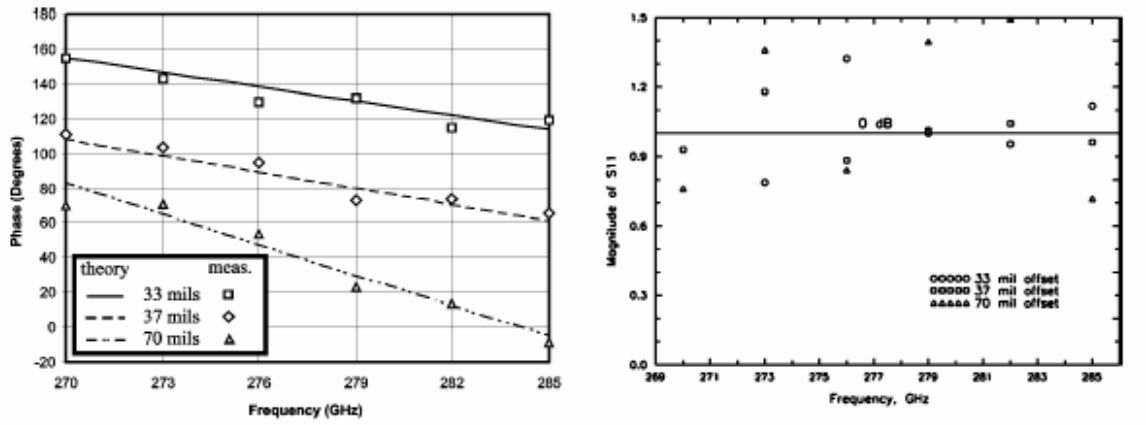

Fig. 12 (a) Measured phase vs. frequency for three offset short circuits. (b) Measured magnitude vs. frequency for three offset short circuits. Also shown is the 0 dB reference for lossless terminations.

Figure 12(a) shows the measured phase of *s*11 for the three offset shorts over the 270 GHz—285 GHz band. The measured phase is close to that predicted using an ideal, lossless short-circuited waveguide as a model and follows the expected slope as a function of frequency. It should be noted that no waveguide losses are accounted for in either the theoretical curves or circuit models used for the calibration standards. Moreover, for these *original* measurements, a mechanically-tuned Gunn diode source was used to drive the multiplier chain. There is approximately a ±5° uncertainty in the phase measurements associated with use of this Gunn diode source and this uncertainty arises from frequency drift of the device as well as manual imprecision in adjusting the micrometers required for frequency tuning. Because the offset shorts used to calibrate the

reflectometer are ideally lossless, the magnitude of the measured reflection coefficient is expected to be near 0 dB. Magnitude measurements performed on the offset shorts are shown in fig. 12(b). In general, the measurements for each shim average near the expected 0 dB, but some data deviate substantially, indicating significant measurement error. Several potential sources of error exist in this prototype instrument and are likely responsible for this. These include imprecise modeling of the calibration standards (which neglects loss), repeatability in connecting the waveguide flanges, and the low power levels detected by the diodes.

A Reflectometer Calibration Method Resistant To Waveguide Flange Misalignment

To address the calibration issues note above, a new reflectometer calibration method is described that utilizes four standards: a flush short, two delay shorts with unspecified but different phases, and an open-ended waveguide. The calibration method eliminates the requirement for a precision waveguide matched load which can be problematic to realize at sub-millimeter wavelengths. Importantly, it is shown that the technique is resistant to waveguide flange misalignment, which is among the most serious factors that degrade the calibration accuracy of vector network analyzers operating above 100 GHz. Scaled measurements using this method have been performed in the W-band (75---110 GHz) where it is readily compared to other calibration methods such as thru/reflect/line (TRL) to assess its utility and performance. Measurement results demonstrate the robustness of this new calibration method and have verified it is superior to the commonly utilized short/delayed-short/load (SDL) technique with respect to the influence of waveguide flange misalignment. This work was published in the IEEE Transactions on *Microwave Theory and Techniques* in July, 2006.

Vector network analyzers (VNA's) operating up to the WR-3 waveguide band (220---325 GHz) are commercially available today. However, for frequency bands above 100 GHz (where waveguide is the most common transmission medium) their measurement performance is often limited by the fabrication tolerances of calibration standards that are used along with the precision with which the waveguide flanges can be mated. Flange misalignment (illustrated in Fig. 13) resulting from the limited precision of waveguide machining techniques is among the most serious challenges to repeatable and accurate scattering parameter measurements at the upper end of the millimeter-wave spectrum. In fact, waveguide flange misalignment can often be as large as 100 μm with standard machining and 65 μm using precision fabrication methods.

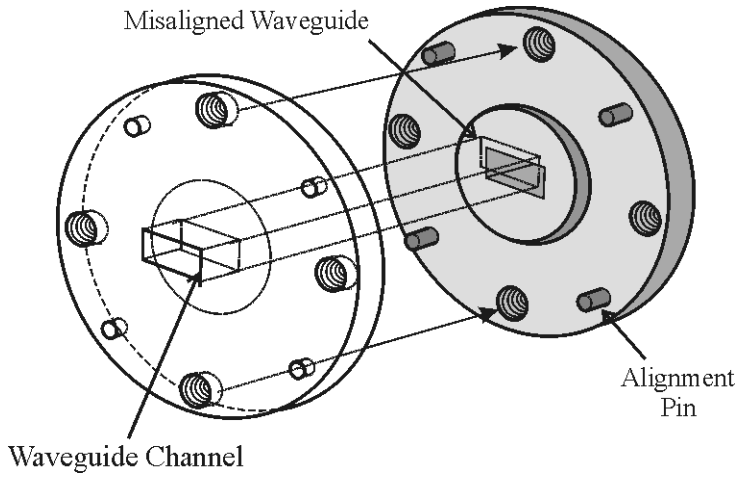

Fig. 13 Illustration of waveguide flange misalignment due to limited machining tolerances and fabrication errors associated with alignment pins and holes.

Flange misalignment can limit the calibration accuracy of VNA's in several ways. Foremost, misalignment can result in a significantly degraded return loss for waveguide matched terminations. As an illustrative example, HFSS simulation has shown a return loss as low as 17 dB of a WR-3 waveguide matched load that is misaligned with the test port by 76 μm along the waveguide E-plane. Misalignment of waveguide flanges can also result in considerable phase error in the response of high-reflection loads (such as delay shorts) that are used as calibration standards. HFSS simulation has also been performed on a WR-3 waveguide quarter-wavelength offset short that is misaligned to the test port by 76 μm along the E-plane. In this case the phase error exceeds 20°. Finally, flange misalignment can also cause the "thru" and "line" standards used in the "thru/reflect/line" (TRL) calibration technique to be mismatched to the test ports, resulting in substantial degradation of calibration accuracy.

Due to the scarcity of verification standards for frequencies above 100 GHz, the new calibration technique was demonstrated and assessed in the W-band (75---110 GHz) where alternative calibration methods such as TRL can be used as a basis for comparison. The distance between the measured and TRL-referenced data on the Γ-plane, ΔΓ, is calculated and plotted in Fig. 14 for different calibration methods. ΔΓ is defined as: $\Delta\Gamma = |\Gamma - \Gamma_{TRL}|$, where Γ is the measured reflection coefficient and Γ_{TRL} is the reflection coefficient corrected using the TRL calibration data. The robustness of the new method and its superiority to the commonly utilized SDL under the influence of waveguide flange misalignment have been demonstrated.

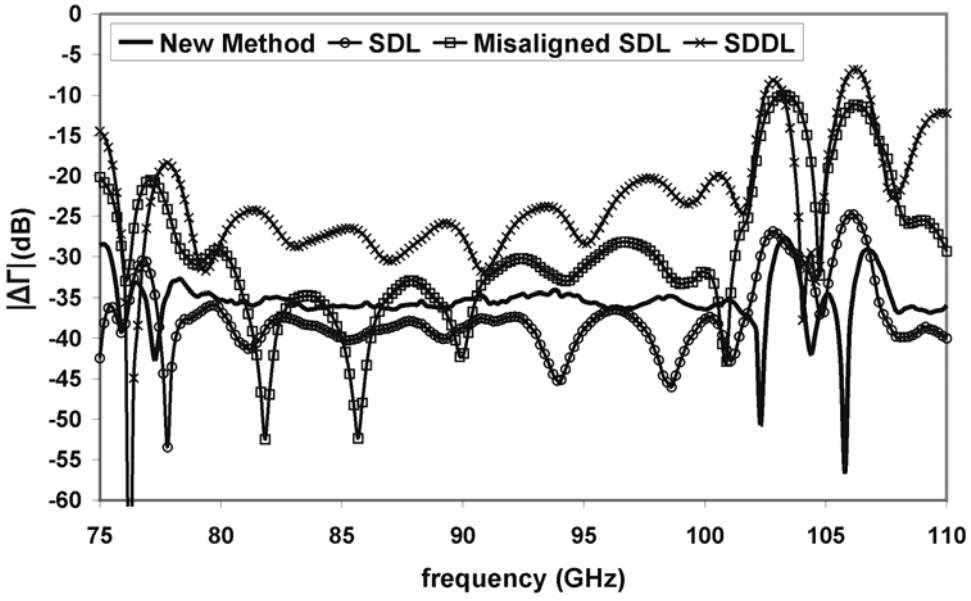

Fig. 14. ΔΓ (dB) versus frequency for an E-H waveguide tuner using different calibration methods. The *new method*, *Misaligned SDL* and *SDDL* are under the influence of waveguide flange misalignment. (The *SDDL method* was proposed by other researchers and utilizes a short, two delay shorts and a matched load.)

Measurement Fixtures for Calibrated Measurements of Biological Materials

Summary:

Knowledge of material parameters, such as complex permittivity, is often desired in applications such as chemical and biological spectroscopy. A relatively simple measurement scheme for permittivity was proposed by Nielsen, who solved the scattering problem for a dielectric post placed in the center of a waveguide and aligned along the E-plane. Moreover, an accurate and general theory for such a measurement scheme has been developed by Leviatan. In this work, these methods are adapted to a one-port measurement system for characterizing biological materials that makes use of a calibration method designed to improve measurement accuracy and significantly reduce system complexity.

The measurement scheme we adopt from Nielsen is shown in Fig. 15, where the sample biological material is placed inside a quartz tube with inner diameter of 0.8 mm. A waveguide short circuit is placed at quarter wavelength from the tube and the reflection coefficient of the system is measured. With proper calibration, the effects of the waveguide fixture can be removed and the complex permittivity of the sample material derived from the measurement. The test fixture was fabricated for one-port measurements in a *W*-band waveguide (75–110GHz). The constitutive parameters of the material in the tube are determined by fitting the complex permittivity to obtain a best fit between the calculated and the measured reflection coefficients.

Typical one-port calibration methods (such as the short/open/load technique) cannot remove errors associated with unrepeatable or imperfect connections between the waveguide test fixture and the network analyzer test port. Thus, an in-situ calibration method is introduced in which the test fixture remains connected to the network analyzer test port for both the calibration and material measurement. As with standard one-port calibrations, three standards are chosen; in this case, an empty waveguide, an empty quartz tube inserted in the waveguide, and a metal (gold-coated) rod inserted in the waveguide.

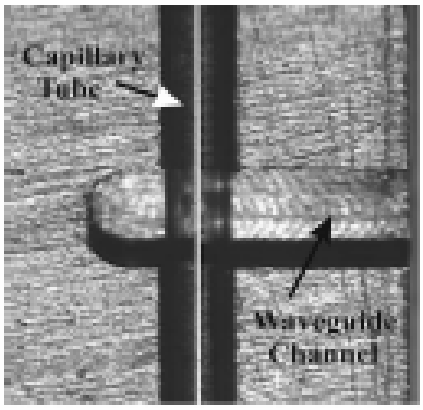

(a)

Frequency (GHz)	Complex permittivity (new calibration)
75	9.8500 - 8.2500i
80.075	8.4800 - 9.9400i
90.05	7.3800 - 6.3600i
94.95	7.3400 - 4.9400i
110	9.6100 - 1.9900i

(b)

Fig. 15. (a) Photograph of the waveguide test fixture with quartz capillary tube. (b) Permittivity of Escherichia coli as found with the new calibration method.

Measurements

The calculated complex permittivity of Escherichia coli cell with solution concentration of 1 mg/ml based on the measurement with the new calibration procedure at 25 C is given in figure 15(b). The validity of the new calibration method was assessed by measuring deionized water as a control. Comparison of the calibrated measurements with other available reference values shows that the measured permittivities are close with slight discrepancies between the imaginary parts. This is attributed to limitations in the present fixture model which does not account for fringing fields that may extend in the tube beyond the boundary of the rectangular waveguide.

Integrated Diode Phase-Shifters for Sideband Generation at Submillimeter Wavelengths

Background and Objective:

This effort was aimed at developing broadband tunable submillimeter-wave sources based on sideband generation. The most efficient sideband generators are constructed from phase-shifters capable of producing a 180 degree phase-shift of the incident signal. The resulting sidebands from the phase modulation can be tuned over a broad frequency range and used as a scanned source for spectroscopic measurements.

Summary and Findings:
The phase shifter investigated in this study is based on a well-known balanced architecture consisting of a 3-dB 90 hybrid and a pair of identical reflective terminations. These terminations are realized with integrated Schottky barrier varactors with device parameters designed to yield a reasonable tradeoff between bandwidth, insertion loss, and amplitude balance. The operating band of this prototype is chosen as 170–260 GHz (waveguide designation WR-4) to permit measurement and characterization using commercially available instrumentation. Furthermore, the circuit is designed to yield a 180 phase shift over its operating band, a requirement for efficient sideband generation.

The phase-shifter circuit consists of four basic components, i.e., (1) a pair of waveguide-to-microstrip transitions; (2) a hybrid coupler; (3) a pair of varactor diodes; and (4) a pair of impedance transformers. Fig. 16(a) shows a photograph of the completed phase-shifter circuit mounted in a WR-4 (170–260 GHz) waveguide housing. Dimensions (in micrometers) of the various components are given in Fig. 16(b). The system characteristic impedance is 100 Ohms and the impedance transformer between the diodes and hybrid is designed to have an impedance ratio of 2. Fused quartz is chosen as the substrate material due to its low cost, rigidity, relatively low dielectric constant, and to permit monolithic integration of GaAs varactor diodes using a substrate bonding process developed at the University of Virginia.

Performance of the integrated phase shifter was characterized and evaluated using an HP8510C vector network analyzer with Oleson Microwave Laboratories (OML) Inc.'s millimeter-wave extension units.2 The OML extension units cover the 140–325-GHz range in two standard waveguide bands, WR-5 (140–220 GHz) and WR-3 (220–325 GHz). Consequently, the measurements presented below represent a concatenation of the measurements performed over both bands. It should be noted that these measurements include the small junction mismatch between the WR-3 and WR-5 flanges of the OML extension modules and the WR-4 flange of the phase shifter. Based on simulations using HFSS, the return loss associated with this mismatch is estimated to be no worse than 20 dB.

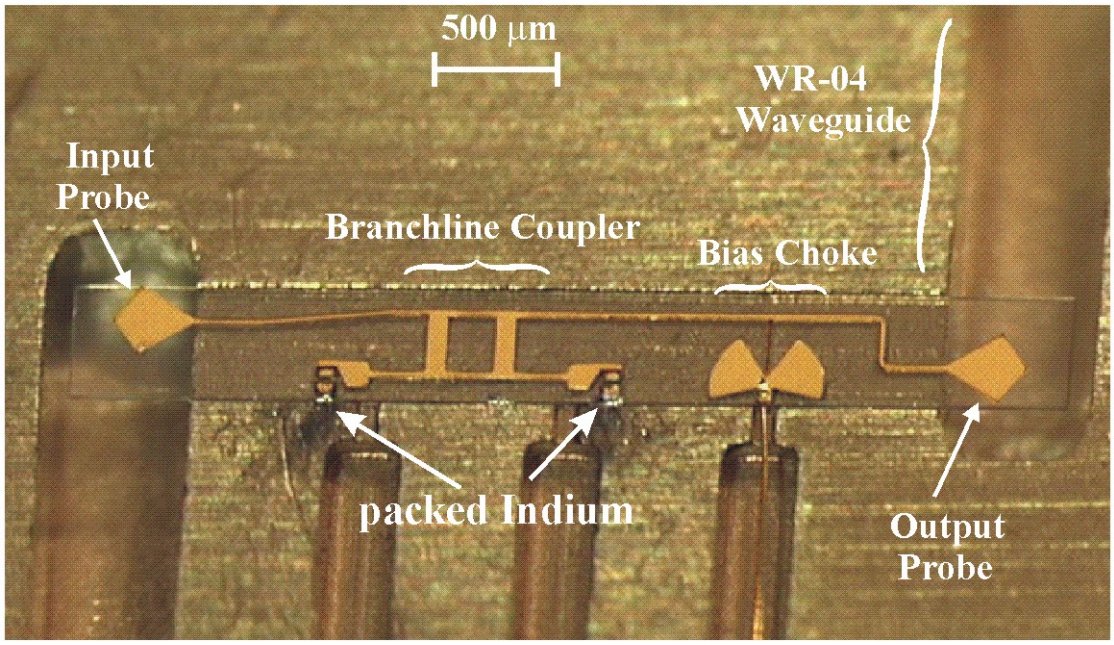

(a)

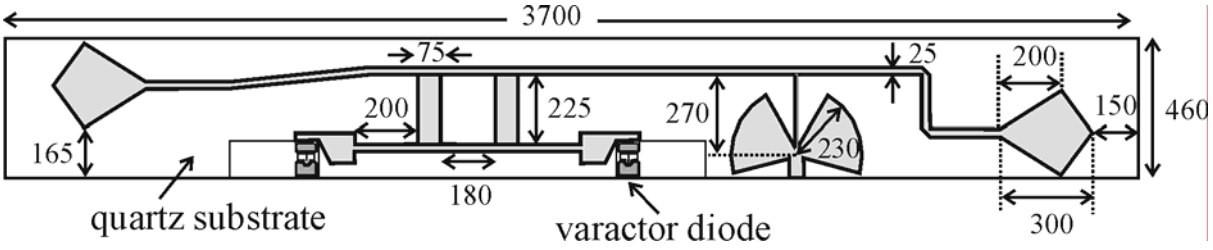

(b)

Figure 16. (a) Photograph of the phase-shifter chip mounted to the waveguide block. (b) Diagram of the phase-shifter chip layout.

Fig. 17 compares the measured response of the circuit with the smallest phase variation with that predicted using Agilent's ADS software. Over a range of 195–250 GHz, the measured phase error (referred to 180 degrees) is less than 15°. Differences between the measured and predicted phase response for the circuit can be attributed to several factors, including variations between the Schottky diodes and errors in placement of the circuit module within the waveguide channel. Fig. 18 shows the insertion and return losses of the phase shifter measured from 190 to 250 GHz. The *average* insertion loss is approximately 5.5 dB over a 40-GHz band (200–240 GHz) and the amplitude imbalance between the "on" and "off" states is better than 0.5 dB between 220–240 GHz.

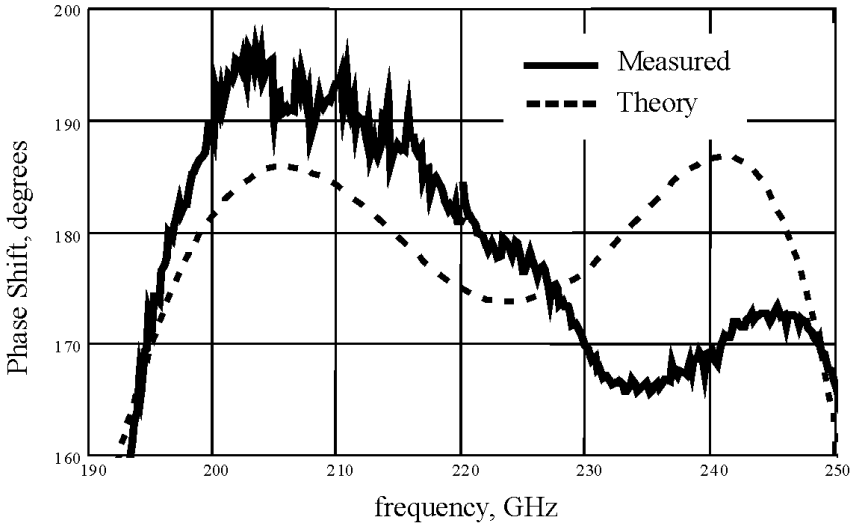

Figure 17. Measured phase shift between the diode "on" and "off" states from 190 GHz to 250 GHz.

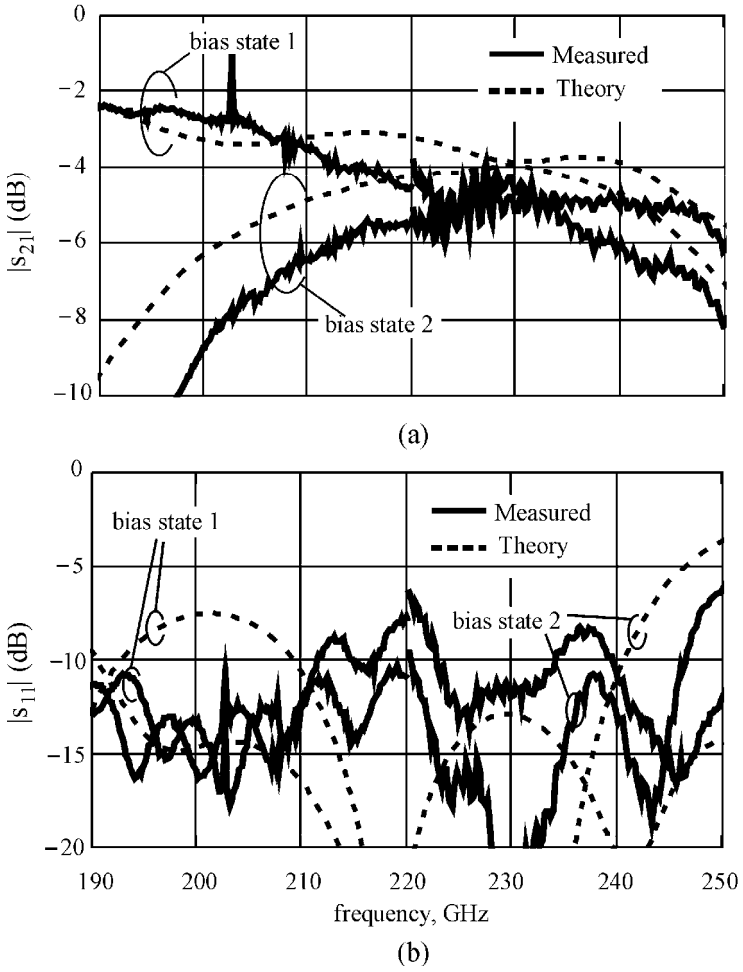

Figure 18. (a) Measured insertion loss (a) and return loss (b) for the phase shifter under both diode bias conditions ("on" and "off") over the 190 to 250 GHz frequency range

Scientific Personnel Supported on this Project:

Faculty	Graduate Research Assistants and Associates
Prof. Robert M. Weikle, II	Dr. Zhiyaing Liu (GRA and post-doc)
Prof. Thomas W. Crowe	Li Yang (GRA)
Prof. Jeffrey L. Hesler	Dr. Sadık Űlker (GRA and post-doc)
	Heng Liu (GRA)

Publications Resulting from this Research:

Refereed Journals

H. Xu, G.S. Schoenthal, J.L. Hesler, T.W. Crowe, and R.M. Weikle, II, "Non-Ohmic Contact Planar Varactor Frequency Upconverters for Terahertz Applications," to be published in the *IEEE Trans. Microwave and Tech.*, April 2007.

H. Xu, Y. Duan, J.L. Hesler, T.W. Crowe, and R.M. Weikle, II, "Subharmonically-pumped millimeter-wave upconverters based on heterostructure barrier varactors," *IEEE Trans. Microwave Theory and Tech.*, vol. MTT-54, no. 10, pp. 3648—3653, October 2006.

Z. Liu and R.M. Weikle, II, "A high-order subharmonic mixer architecture using a phased local oscillator," *IEEE Trans. Microwave Theory and Tech.*, vol. MTT-54, no. 7, pp. 2977―2982, July 2006.

Z. Liu and R.M. Weikle, II, "A reflectometer calibration method resistant to waveguide flange misalignment," *IEEE Trans. Microwave Theory and Tech.*, vol. MTT-54, no. 6, pp. 2447—2452, June 2006.

Z. Liu and R.M. Weikle, II, "A Compact Quadrature Coupler Based On Coupled Artificial Transmission Lines," *IEEE Microwave and Wireless Components Lett.*, vol. 15, no. 12, pp. 889—891, December 2005.

T.W. Crowe, W.L. Bishop, D.W. Porterfield, J.L. Hesler and R.M.Weikle, II, "Opening the Terahertz Window with Integrated Diode Circuits," (invited) *IEEE Journal of Solid-State Circuits*, vol. 40, no. 10, pp. 2104—2110, Oct. 2005.

Z. Liu, J.C. Midkiff, H. Xu, T.W. Crowe, and R.M.Weikle, II, "Broadband 180° Phase-Shifters Using Integrated Submillimeter-Wave Schottky Diodes," *IEEE Trans. Microwave Theory and Tech.*, vol. MTT-53, no. 9, pp. 2949—2955, Sept. 2005.

R.M. Weikle, II, T.W. Crowe, and E.L. Kollberg, "Multiplier and Harmonic Generator Technologies for Terahertz Applications," *Internat. Journal of High Speed Electronics and Systems* (World Scientific Publishing Co.), vol. 13, no. 2, 429―456, 2003.

Major Conference Proceedings

D. Hui and R.M. Weikle, II, "Calibration of six-port reflectometers using null double injection," *67th ARFTG Microwave Measurement Conference Digest*, San Francisco, CA, pp. 164—179, June 2006.

Z. Liu and R.M.Weikle, II, “A 180° Hybrid Based On Coupled Asymmetrical Artificial Transmission Lines," *2006 IEEE Int. Microwave Symposium Digest*, San Francisco, CA, pp. 1555—1558, June 2006.

H. Xu, Z. Liu, C.H. Smith, III, J.L. Hesler, B.S. Deaver, Jr. and R.M. Weikle, II, “A Non-Contacting Tunable Waveguide Backshort for Terahertz Applications," *2006 IEEE Int. Microwave Symposium Digest*, San Francisco, CA, pp. 1919—1922, June 2006.

L. Yang, T. Kotchiev, Z. Liu, and R.M. Weikle, II, “New calibration method for measuring permittivity of biological material with W-band waveguide," Proceedings of the *Joint 31st International Conf. On Infrared And Millimeter Waves and the 14th International Conference On Terahertz Electronics*, Shanghai, China, p. 408, September 2006.

R.M. Weikle, II, Z. Liu, L. Yang, S. Űlker, and A.W. Lichtenberger, “Sampled-Line Reflectometers for Terahertz *s*-Parameter Measurements," *Proceedings of the SPIE*, Conference 5790, Terahertz for Military and Security Applications III, Orlando, FL, pp. 137—148, March 2005.

R.M. Weikle, II, Z. Liu, Heng Liu, Lei Liu, S. Űlker, A.W. Lichtenberger, “Six-port reflectometers for terahertz scattering parameter measurements using submillimeter wavelength detectors," *Proceedings of SPIE*, Conference 5592 on Nano-Fabrication: Technologies, Devices and Applications, Philadelphia, PA, pp. 328—340, October 2004.

Z. Liu, J.C. Midkiff, and R.M. Weikle, II “Millimeter-Wave Phase Shifters Utilizing Planar Integrated Schottky Barrier Diodes," *2003 IEEE Int. Microwave Symposium Digest*, Philadelphia, PA, pp. 2241—2244, June 2003.

H. Xu, J.L. Hesler, Y. Duan, T.W. Crowe, and R.M. Weikle, II “A Heterostructure Barrier Varactor Sideband Generator," *2003 IEEE Int. Microwave Symposium Digest*, Philadelphia, PA, pp. 2031—2034, June 2003.

S. Űlker, R.M. Weikle, II, “Submillimeter-Wave Scattering Parameter Measurements With A Sampled-Line Six-Port Reflectometer," *60th ARFTG Conference Digest*,Washington D.C., pp. 71—80, December 2002.

References for this Report

[i] A. Driks, "Bacillus subtilis Spore Coat" Microbiology and Molecular Bio. Revs., March 1999, pp. 1-20.

[ii] B. Yu, A. Alimova, A. Katz, nd R. R. Alfano "THz Absorption Spectrum of Bacillus subtilus spores," Proc. SPIE, paper 5727-3, 2005.

[iii] C.F. Bohren and D.R. Huffman, *Absorption and Scattering of Light by Small Particles*, (Wiley, New York, 1983).